NSF/RA-800428

PB81-168296

CIVIL ENGINEERING STUDIES

STRUCTURAL RESEARCH SERIES NO. 486

EFFECTIVE WIDTH OF FLOOR SYSTEMS FOR APPLICATION IN SEISMIC ANALYSIS

by

F. S. COTRAN

and

W. J. HALL

A Technical Report of
Research Supported by the
NATIONAL SCIENCE FOUNDATION
under Grant Nos. ENV 77-07190
and
PFR 80-02582

DEPARTMENT OF CIVIL ENGINEERING
UNIVERSITY OF ILLINOIS
AT URBANA-CHAMPAIGN
URBANA, ILLINOIS

NOVEMBER 1980

INFORMATION RESOURCES
NATIONAL SCIENCE FOUNDATION

EFFECTIVE WIDTH OF FLOOR SYSTEMS FOR APPLICATION IN SEISMIC ANALYSIS

by
FADI SHAFIC COTRAN
and
WILLIAM J. HALL

A Report on a Research Project Sponsored by the
NATIONAL SCIENCE FOUNDATION
Research Grant Nos. ENV-07190 and PFR-80-02582

UNIVERSITY OF ILLINOIS
Urbana, Illinois
November 1980

ACKNOWLEDGMENT

This report is based on the doctoral dissertation of Fadi S. Cotran submitted to the Graduate College of the University of Illinois at Urbana-Champaign in partial fulfillment of the requirements for the degree of Doctor of Philosophy in Civil Engineering. The research was directed by William J. Hall and David A. W. Pecknold, Professors of Civil Engineering, and was supported by the National Science Foundation (RANN) under Grant Nos. ENV 77-07190 and PFR 80-02582. The above noted support is gratefully acknowledged.

The numerical results were obtained using the computer program FINITE developed by Professor Leonard A. Lopez and colleagues at the Civil Engineering Department.

The computation was performed on the Burroughs B6700 computer system of the Civil Engineering Systems Laboratory and the CDC Cyber/175 computer system of the Computing Services Office of the University of Illinois at Urbana-Champaign.

Any opinions, findings, and conclusions or recommendations expressed in this report are those of the authors and do not necessarily reflect the views of the National Science Foundation.

TABLE OF CONTENTS

Page

1. INTRODUCTION ---------- 1

1.1 Background ---------- 4
1.2 Purpose of Study ---------- 6
1.3 Scope of Investigation ---------- 6
1.4 Notation and Units ---------- 7

2. ANALYTICAL STUDY ---------- 10

2.1 Equivalent Composite Stiffness ---------- 11
2.2 Deriving Effective Width Ratios ---------- 16
2.3 Finite Element Analysis ---------- 19
2.3.1 Mesh ---------- 20
2.3.2 Elements ---------- 22
2.3.3 Constraints ---------- 24
2.3.4 Loading ---------- 24

3. RESULTS ---------- 25

3.1 Variation of Parameters ---------- 25
3.1.1 Flexural Effective Width ---------- 25
3.1.2 Axial Effective Width ---------- 27
3.2 Discussion of Accuracy ---------- 28
3.3 Proposed Method for Using the Effective Width Coefficients -- 30
3.4 Remarks on Applicability ---------- 32

4. EXAMPLE APPLICATIONS ---------- 34

4.1 Composite Member Properties of a Slab ---------- 35
4.2 Seismic Analysis of a Frame ---------- 39
4.2.1 Gravity Loads ---------- 40
4.2.2 Equivalent Composite Beam Properties ---------- 40
4.2.3 Modal Analysis ---------- 41
4.3 Concluding Remarks on Seismic Analysis ---------- 50

REFERENCES ---------- 52

LIST OF TABLES

Table		Page
3.1	Flat Slab Stiffness, $M/E_s\theta_o$, for Varying Aspect Ratio, L_1/L_2, and Longitudinal Relative Column Size, c_1/L_1	56
3.2	Flat Slab Stiffness, $M/E_s\theta_o$, for Varying Aspect Ratio, L_1/L_2, and Transverse Relative Column Size, c_2/L_2	57
3.3	Composite Stiffness, $M/E_s\theta_o$, for Varying Aspect Ratio, L_1/L_2, and Longitudinal Relative Column Size, c_1/L_1	58
3.4	Composite Stiffness, $M/E_s\theta_o$, for Varying Aspect Ratio, L_1/L_2, and Transverse Relative Column Size, c_2/L_2	59
3.5	Flexural Effective Width Coefficients, λ_{f_o}, for Varying Aspect Ratio and Longitudinal Relative Column Size	60
3.6	Correction Factors for Flexural Effective Width Coefficients, λ_f/λ_{f_o}, for Varying Aspect Ratios and Transverse Relative Column Size	61
3.7	Axial Effective Width Coefficients, λ_{a_o}, for Varying Aspect Ratios and Longitudinal Relative Column Size	62
3.8	Correction Factors for Axial Effective Width Coefficients, λ_a/λ_{a_o}, for Varying Aspect Ratios and Transverse Relative Column Size	63
3.9	Composite Stiffness for Varying Slab Aspect Ratio	64
3.10	Composite Stiffness for Varying Relative Column Dimension	65
3.11	Composite Stiffness for Varying Beam Eccentricity	67
3.12	Composite Stiffness for Varying Slab Thickness	69

Table Page

3.13 Composite Stiffness for Varying Beam Area ---------- 70

3.14 Composite Stiffness for Varying Beam Moment of Inertia, I_{BT} ---------- 71

3.15 Composite Stiffness for Various Values of Controlling Parameters ---------- 72

LIST OF FIGURES

Figure		Page
2.1	Composite Section	73
2.2	Composite Beam in Antisymmetric Deflection	74
2.3	The 16x16 Finite Element Mesh	75
2.4	The 10x10 Finite Element Mesh	76
2.5	The 3x25 Finite Element Mesh	77
2.6	Comparison of the Deflected Shape of the Composite Beam for Different Finite Element Meshes	78
2.7	Degrees of Freedom of the 16 Node Rectangular Plate Bending Element	79
2.8	Generalized Stress and Strain Resultants for the Rectangular Plate Bending Element	80
2.9	Degrees of Freedom of the Plane Stress Rectangle	81
2.10	Generalized Stresses and Strains for the Plane Stress Rectangle	81
2.11	Typical Interior Panel	82
3.1	Flexural Effective Width Ratios	83
3.2	Correction Factors for Flexural Effective Width Ratios	84
3.3	Axial Effective Width Ratios	85
3.4	Correction Factors for Axial Effective Width Ratios	86
4.1	Three-story Frame	87
4.2	Lateral Stiffness Coefficients	88
4.3	Response Spectrum Used in Example 2	89

1. INTRODUCTION

The analysis of building frames is one of the major tasks that a structural engineer faces in order to properly design the members composing the frame. The structure is analyzed for all the loadings desired and the members are subsequently designed to resist the anticipated forces with provision for margin of safety, along with other factors such as deflection control, durability, and ductility, to name a few.

The adequacy of such an analysis as a part of the design process depends in part on the accuracy of the properties chosen for the various members of the frame, the assumptions of the analysis approach employed, as well as the reasonableness of the various loadings considered. Since the properties of the structural members are not known until they are designed, and since they cannot be proportioned accurately before the frame is analyzed, it obviously becomes a matter of iteration to obtain a satisfactory and economical design. For a given functional structural form and selected loadings, properties must be assumed to be able to analyze the frame for a first trial. Thereafter, members can be proportioned and if large discrepancies exist between the assumed and obtained properties, the frame is reanalyzed with the new properties of its structural members. Usually, there would be no need to reanalyze more than once or possibly twice to obtain a satisfactory design if the initial assumptions were reasonable. It is evident that member properties are a vital input to frame analysis.

Dynamic loadings, such as those arising from earthquakes, present a unique problem in structural analysis. These forces arise from the

occurrence of natural hazards that are less predictable than the deterministic gravity loads. A structure subjected to ground acceleration will have inertial forces that depend on mass, and its dynamic response will depend on the combination of stiffness and mass, among other factors. The frame is subjected to lateral forces, and must resist these forces in addition to the gravity loads imposed on it. For strong earthquakes the resulting lateral forces induce stresses in the structural members that may be considerably larger than those arising from gravity loads. The structure must be designed to resist these forces in combination with the gravity loads.

The structural members that are normally assumed to resist the dynamic lateral loads are the columns, beams, shear walls, and lateral bracing, depending on the type of building being analyzed. Floor systems, the subject of this study, have consistency been neglected in most types of dynamic analyses of frames. This study presents a simplified method for determining the effective width of floor systems (with or without supporting beams) for use in analysis of frames subjected to lateral forces. The results are based on a parametric study performed using linear elastic finite element analysis of typical interior panels.

There are many reasons for this situation, some of which are warranted, while others are not. The main reasons for neglecting the resistance of floor systems against dynamic loads are the following:

(1) The lateral forces are usually resisted by the stiffest members, usually the moment resisting frame, the shear wall, or lateral bracing. Therefore, whatever added lateral strength the floor system may offer will be on the conservative side, and its

assumed small contribution does not warrant the added effort necessary to consider its effect.

(2) Floor system types are diversified, and their behavior differs. Therefore, generalization is difficult.

(3) Meticulous consideration of the stiffness of the floor system requires three dimensional dynamic finite element analysis which makes the problem prohibitive in computational time. Although computer programs capable of such an analysis are available [7, 29, 30]*, the number of elements required is large, rendering the analysis either impossible or extremely expensive.

(4) Few experimental results are available for framed systems employing loadings of the type considered herein, especially frame systems with floors.

Traditionally, the functional performance requirements of a floor system usually include: 1) adequate strength and stiffness to safety support dead loads and live loads without excessive deflection, 2) provision for lateral support of walls, 3) satisfactory resistance to transmission of airborne and structure-borne sound, 4) suitable fire resistance, 5) suitability for application of finish materials, 6) adaptability to economical methods of assembly and erection, 7) space to accommodate heating, air conditioning, electrical, and plumbing equipment, and 8) control of heat loss and the flow of water vapor. None of these requirements includes resistance to seismic forces.

---

* Numbers in brackets refer to citations in the list of references.

One of the most important reasons for taking the floor slab into consideration is the fact that it must deform together with the beams which support it; consequently, the floor system will affect the stiffness, strength, ductility, and energy dissipation characteristics of the frame. This is especially true in critical regions like column-beam-slab connections.

Underestimating or neglecting the effect of the floor slabs on the strength of the girders may change an assumably balanced design to a design with columns that are not capable of resisting the moment that can be developed by the existing girders acting compositely with the slab under lateral loads. As a result, the critical overstressed region will develop in the columns. This type of behavior could be undesirable because the columns may have less available ductility than the beams; therefore, the idea of "soft story deformation" or a balanced-type design will not be fulfilled in such a case.

1.1 Background

One of the early studies dealing with composite structural action between slabs and beams [26] was concerned with the encasement of steel beams with concrete. Later, composite beams consisting of concrete slabs on structural steel I-beams were investigated [10], and the recommendation was offered that they be designed on the basis of a homogeneous section wherein the concrete area is transformed into an equivalent area of steel.

The necessary information required for such calculations involved knowledge of the area of the slab to consider for composite action. Early theoretical studies attempted to provide rational values for the effective

widths of floor slabs in composite action [20, 22, 35, 40]. Recent analytical studies on the representation of floor systems can be grouped into three types.

(1) ACI Equivalent Frame Method [3, 4, 12, 13, 18]. This method was derived for gravity loading, and is based on modeling a slab structure as an equivalent frame, and taking the beams as the portion of slab bounded by the midspan centerline in each direction. The column stiffness is modified, and columns are assumed fixed at their far ends. Methods for extending this method for lateral loads have been proposed recently [33, 39].

(2) Effective Slab Width [1, 9, 21, 27, 34]. This method assumes a certain width of slab to be effective in being considered as an equivalent beam acting compositely with the beam supporting it. Several suggested methods are available for computing the effective width. Some researchers suggested a specific value of the effective width while others suggested different values for different slab dimensions.

(3) Stiffness Modification [28]. This method modifies the stiffness matrix of the beam without identifying a physical shape for the slab. The resulting modified stiffness matrix is claimed to account for the slab stiffness under gravity loads.

There were also some other studies conducted that included analytical investigation of other behavioral characteristics of the slab [2, 8, 14 - 17, 19, 23, 25, 36, 37, 41 - 43]. To the best of the author's knowledge, there is only one set of unpublished experimental test results dealing with flat plate multistory unbraced structures tested by the National

Research Council of Canada as described in Ref. 39. This fact makes it quite difficult to compare the proposed methods of analysis to actual tested behavior.

Most of the studies performed dealt primarily with flat slabs, and the effect of the existence of a supporting beam (steel or concrete) has not been adequately investigated. Furthermore, behavior of the composite sections under lateral loads leads to a complex problem. As a result, in part, because the contribution has been felt to be small, it has been customary to neglect the floor contribution.

1.2 Purpose of Study

The purpose of this study is to develop a rational and simple method using elastic beam theory for calculating the effective width of floor systems for use in analyzing frames subjected to lateral loading.

The method described covers a wide range of practical values of the slab dimensions. The analytical method can be applied to both steel and concrete frames and to cases of flat slabs as well as slabs with supporting beams.

1.3 Scope of Investigation

The investigation is based on a parametric study of typical interior panels of floor systems, with and without supporting beams, using elastic finite element analysis to model the behavior of the floor system when frame is subjected to lateral loads.

Chapter 2 deals with the theoretical derivation of the method and the procedure employed for the finite element analysis. In Chapter 3, the results obtained and the proposed simplified method of analysis for

estimating the composite properties are presented. Some simple examples illustrating application of the proposed method, with emphasis on seismic analysis and the resistance of floor systems under dynamic loads, are presented in Chapter 4.

1.4 Notation and Units

All units of the quantities used in this study are consistent units of force, length, and time. The quantities must be used in this manner throughout this report.

A = spectral amplification factor for peak ground acceleration

A_B = cross-sectional area of beam

A_{BT} = transformed cross-sectional area of beam

A_{se} = effective area of slab

A_{sg} = gross area of slab

c_1 = column dimension in loading direction

c_2 = column dimension in transverse direction

d = depth of beam

D = spectral amplification factor for peak ground displacement

e = distance between the neutral axes of slab and beam

E_B = modulus of elasticity of the beam

E_s = modulus of elasticity of the slab

f_i = the ith natural frequency of vibration

$\{f_{sn}\}$ = lateral story forces of the nth mode

$\{f_{s,max}\}$ = maximum lateral story forces when they are combined by the method of square root of the sum of the squares of the modal story forces

f'_c = concrete 28-day compressive strength

g = gravitational acceleration

I_B = moment of inertia of beam

I_{BT} = transformed moment of inertia of beam

I_{eq} = equivalent moment of inertia of the composite section

I_{eq_1} = equivalent moment of inertia of the slab

I_{eq_2} = equivalent moment of inertia of slab and beam compositely

I_{se} = effective moment of inertia of the slab ($I_{se} = \lambda_f I_{sg}$)

I_{sg} = gross moment of inertia of the slab

$I_T = \lambda_f I_{sg} + I_{BT}$

$[K]$ = stiffness matrix for lateral displacements

L_1 = longitudinal span

L_2 = transverse span

m = mass

$[m]$ = lumped mass matrix

M = bending moment at column centerline

M' = bending moment at end of the free span of the beam

M_{beam} = maximum bending moment acting on the beams in the frame

$M_{col.}$ = maximum column moment in the frame

n = modular ratio ($n = E_B/E_s$)

P = axial load on column

P' = equivalent axial load for bending moment on column

$P_{col.}$ = maximum column axial load in the frame

S_{an} = spectral acceleration at the nth mode of vibration

t = thickness of slab

u = displacement along the x-axis

v = displacement along the y-axis

V = spectral amplification factor for peak ground velocity

$V_{b,max}$ = maximum base shear computed by the method of square root of the sum of the squares of the modal base shears

V_{b_n} = base shear for the nth mode of vibration

w = vertical displacement along the z-axis

$w_{,xyz}$ = derivative of w with respect to x, y, z, etc.

y = distance between the composite neutral axis and neutral axis of the slab

α_n = participation factor of the nth mode of vibration

θ_o = end rotation of composite section

θ_y = rotation about the y-axis

θ_z = rotation about the z-axis

λ_a = axial effective width ratio

λ_{a_o} = axial effective width ratio for $c_2/L_2 = 0.06$

λ_f = flexural effective width ratio

λ_{f_o} = flexural effective width ratio for $c_2/L_2 = 0.06$

$\{\phi_n\}$ = the nth mode shape vector

ν = Poisson's ratio

ω = circular frequency of vibration

2. ANALYTICAL STUDY

The behavior of a slab in a frame subjected to lateral loading is complex. The complexity is compounded by the presence of a flexible beam helping the slab. Part of the complexity arises because the beam is usually eccentric with respect to the slab, i.e., the beam's neutral axis usually lies at some distance below that of the slab.

This study is directed at analyzing typical interior panels of frames that are subjected to lateral forces. The interior panels considered in the analysis may have supporting beams in the longitudinal direction (loading direction). The proposed hypothesis is that there are two nondimensional constants for a given slab aspect ratio and relative column size which model the stiffness of the slab to that of an equivalent beam. These two constants are assumed to be properties of the slab shape and do not depend on the shape or properties of the supporting beam. This equivalent beam is assumed to act in full composite action with the supporting beam, if it exists. Therefore, the effect of the eccentricity is incorporated in the equations of composite action analytically. The two constants that govern the equivalence of the stiffness of the slab to that of the equivalent beam modify the gross moment of inertia and the gross area of the slab for use in determining the composite properties of the section.

Several major assumptions were made in this study and are as follows:

(1) Behavior of all materials of the members being analyzed is elastic and follows Hooke's law.

(2) There is no slippage between the slab and the flexural beam at their interface. Bonding is assumed to be ideal and full composite

action is developed. In practice, in order to make this assumption valid, shear connectors normally would be provided between the slab and the steel beam. In reinforced concrete frames, the slab and beam normally would be cast monolithically in order to make this assumption valid.

(3) There is no relative displacement between adjacent frames of the building in the direction of loading.

(4) Column midheights are points of inflection in lateral deflection of the frame.

(5) Column lines and slab midspan centerlines in the longitudinal direction (direction of loading) are lines of symmetry.

(6) Column lines and slab midspan centerlines in the transverse direction are lines of antisymmetry.

(7) The area of slab bound by the column has infinite stiffness and deflects as a rigid body.

2.1 Equivalent Composite Stiffness

Composite action is developed when two structural members such as a concrete floor system and the supporting steel beams are integrally connected and deflect as a single member. The development of composite action is insured if strain distribution is continuous over the entire cross section.

When a system acts compositely, no slippage occurs between the slab and beam. Horizontal shear forces are developed at the surface between the slab and beam. There should be enough friction and shear reinforcement at the slab-beam interface to insure proper shear transfer so that full composite action is developed. If slippage occurs, the moment capacity of the

composite section is reduced. The following analysis assumes no slippage at the slab-beam interface.

Simple beam theory was used for the analysis. Figure 2.1 shows a slab supported by a flexural beam. The slab and the beam need not have the same modulus of elasticity. The section properties of the beam can be transformed by the modular ratio,

$$n = \frac{\text{Modulus of elasticity of beam, } E_B}{\text{Modulus of elasticity of slab, } E_s}$$

Stiffness is now referenced to the modulus of elasticity of the slab. The transformed area and moment of inertia of the beam are

$$A_{BT} = n \times (\text{area of beam})$$

$$I_{BT} = n \times (\text{moment of inertia of beam})$$

There exists a certain effective area of slab, A_{se}, and an effective moment of intertia, I_{se}, which if the slab is replaced by a beam having these properties will yield the same end rotation, θ_o, when the frame is subjected to lateral loads. The values of A_{se} and I_{se} are the properties to be determined in order to make the equivalence between the slab and the equivalent beam correct, as far as the overall behavior of this assemblage in a frame is concerned.

The position of the neutral axis of this composite section below the neutral axis of the slab can be easily determined by simple mechanics, and may be expressed by

$$y = \frac{A_{BT}e}{A_{BT} + A_{se}} \qquad (1)$$

The composite moment of inertia of the section is given by

$$I_{eq} = I_{se} + A_{se}y^2 + I_{BT} + I_{BT}(e - y)^2 \tag{2}$$

Simplifying and rearranging terms, one obtains

$$I_{eq} = A_{se}ey + I_{se} + I_{BT} \tag{3}$$

or

$$I_{eq} = \frac{A_{BT}A_{se}}{A_{BT} + A_{se}} e^2 + I_{se} + I_{BT} \tag{4}$$

It is evident that if the effective area and moment of inertia of the slab are known, then I_{eq} can be calculated. A_{se} and I_{se} should be less or equal than the gross sectional properties of the slab, A_{sg} and I_{sg}.

For convenience, A_{se} and I_{se} can be represented as some fraction of the gross properties, namely,

$$A_{se} = \lambda_a A_{sg} \tag{5}$$

and

$$I_{se} = \lambda_f I_{sg} \tag{5a}$$

The terms λ_a and λ_f represent that fraction of the gross area and moment of inertia of the slab, respectively, which if used as properties of an equivalent beam replacing the slab, will yield the same composite stiffness in the frame. These fractions may be referred to as Effective Width ratios, Effective Width coefficients, or Equivalent Beam coefficients. In reality they are merely correction coefficients for equating the action of the slab, as a plate, to that of a beam. Physically, the slab can be thought of as a beam whose depth is equal to the thickness of the slab

and whose width is equal to the effective width ratio times the width of the slab. There are two effective widths to be considered, one for bending action (to determine I_{se} in Eq. (4)), and the other for composite action (to determine A_{se} for the first term of Eq. (4)). Since the two effective widths are determined from the two nondimensional correction constants that satisfy Eq. (4), they are not necessarily equal in general. Earlier in the study, it was assumed that there was a single effective width of slab for usage in Eqs. (4) and (5). However, when the same slab and beam were analyzed with a varying eccentricity, the resulting calculated effective width did not remain constant. The effective width had a maximum value equivalent to what was later determined as λ_f when the eccentricity was zero. As the eccentricity increased, the effective width decreased and reached a minimum value (for large eccentricities) of what was later found to be the value of λ_a. Since the basic assumption was that the effective width is a property of the slab, an effective width dependent on beam properties did not fulfill this assumption. Therefore, the more general approach of assuming that two constants are required to satisfy the proposition of an effective width independent of the properties of the beam was adopted.

In order to calculate effective width coefficients, the stiffness of the slab/beam assemblage must be determined. This stiffness was derived by applying beam theory to the end rotations obtained from finite element analysis of the slab and beam as discussed in Sections 2.2 and 2.3.

Under lateral loading of the frame, the slab/beam will deflect in the antisymmetric manner shown in Fig. 2.2. The finite dimension of the column will make the corner encompassed by the column to be essentially

rigid. The applied end moment, M, caused by the shear in the column will cause an end rotation, θ, as shown in Fig. 2.2. The dimension c_1 represents the column width in the loading direction, which is considered rigid in the foregoing analysis. The equivalent beam is defined as that beam which will have the same end rotation, θ, for the same applied moment, M. Its moment of inertia, I_{eq}, is given by

$$I_{eq} = M'L'/(3E\theta) \tag{6}$$

where $L' = (L_1 - c_1)/2$, M' is the bending moment at the end of the rigid part of the equivalent beam, and θ is the angle shown in Fig. 2.2, given by

$$\theta = \theta_o + \theta_1 \tag{7}$$

For small angles,

$$\theta_1 = 2w/(L_1 - c_1)$$

where the deflection, w, is given by

$$w = \theta_o c_1/2$$

Substitution in Eq. (7) gives

$$\theta = \theta_o/(1 - c_1/L_1) \tag{7a}$$

The bending moment, M', may be written in terms of the applied moment, M, by statics, as

$$M' = M(1 - c_1/L_1) \tag{8}$$

Finally, substitution of Eqs. (7a) and (8) in Eq. (6) gives the expression of the equivalent moment of inertia,

$$I_{eq} = (1/3)(M/E\theta_o)(L_1/2)(1 - c_1/L_1)^3 \qquad (9)$$

If the value of $M/E\theta_o$ is known for a given composite slab and beam, then the moment of inertia of the equivalent beam can be calculated using Eq. (9).

2.2 Deriving Effective Width Ratios

The foregoing derivation assumes that the values of $M/E\theta_o$ for the cases being considered are readily available. These values were obtained by finite element analysis which will be discussed in section 2.3. With the equivalent composite moment of inertia of the slab and beam determined, it is a fairly simple task to calculate the effective widths.

Substitution of Eqs. (5) and (5a) in Eq. (4) and rearranging gives

$$I_{eq} - I_{BT} = \frac{\lambda_a A_{sg} A_{BT}}{\lambda_a A_{sg} + A_{BT}} e^2 + \lambda_f I_{sg} \qquad (10)$$

The flexural effective width ratio may be determined from the equivalent composite moment of inertia for the cases where no beam exists or for the cases where the eccentricity of the beam is zero. Either method should yield comparable results for the flexural effective width ratio, λ_f, which will be given by

$$\lambda_f = (I_{eq_1} - I_{BT})/I_{sg}$$

where I_{eq_1} is obtained using Eq. (9) for the case where no beam is present or when the eccentricity of the beam is zero.

With λ_f determined for the slab under consideration, Eq. (10) can be solved for the axial effective width ratio, λ_a, which gives

$$\lambda_a = \frac{A_{BT}}{A_{sg}} \frac{I_{eq_2} - (\lambda_f I_{sg} + I_{BT})}{\lambda_f I_{sg} + (I_{BT} + A_{BT}e^2) - I_{eq_2}} \tag{11}$$

where I_{eq_2} is the equivalent moment of inertia of the composite section when an eccentric beam is present.

The numerator of the above expression represents the difference between the composite moment of inertia about the composite neutral axis and the sum of the moments of inertia of the beam and the effective flexural width of the slab about their individual neutral axes. The denominator represents the difference between the sum of the effective moment of inertia of the slab and beam about the neutral axis of the slab and the composite moment of inertia about the composite neutral axis.

If the term $(\lambda_f I_{sg} + I_{BT})$ is called the total moment of inertia, I_T, about the individual neutral axes of slab and beam, and rearranging terms, Eq. (11) becomes

$$\lambda_a = \frac{A_{BT}/A_{sg}}{\frac{A_{BT}e^2}{I_{eq_2} - I_T} - 1} \tag{12}$$

Therefore, for a given slab, two values of I_{eq} are needed to calculate λ_f and λ_a. The flexural effective width ratio can be calculated by analyzing the slab without a beam. With the value of λ_f obtained, I_T may be determined by

$$I_T = \lambda_f I_{sg} + I_{BT}$$

In order to calculate the axial effective width ratio, λ_a, an eccentric beam is inserted in the longitudinal direction. With the computed equivalent

composite moment of inertia, I_{eq_2}, obtained from finite element analysis, the value of λ_a can be determined using Eq. (12).

As will be noted later in Chapter 3, it was found from finite element analysis that both effective width ratios are independent of beam properties. The term λ_f depends only on the aspect ratio of the slab, L_1/L_2, and the relative size of the column, c_1/L_1 and c_2/L_2. The thickness of the slab, t, does not affect λ_f.

Although Eq. (12) appears to depend on the properties of the beam, it was found, from analyzing the same slab with various beam properties, that it actually does not have such dependence. The axial effective width ratio, λ_a, remains constant as the area, moment of inertia and eccentricity of the beam are varied. Slight variation in λ_a occurs when extremely small relative values of e, A_{BT}, and I_{BT} are used. Such small values are not likely to be found in practice, and their importance is only of academic interest. In general, if the transformed moment of inertia of the beam, I_{BT} is kept greater than about 5 percent of the gross moment of inertia of the slab, I_{sg}, the effective width ratios do not change. For transformed beam areas, A_{BT}, greater than about one percent of the gross slab area, A_{sg}, the effective width ratios are found to remain constant for a given slab. Beam eccentricities greater than about one-fifth the slab thickness had essentially no effect on the effective widths. The errors introduced by using smaller values of the aforementioned parameters are not large, and it is believed that they arise as a result of round-off error in the numerical solution.

After experimentation with several values of relative beam properties, it was determined that fairly high values avoid any possible round-off

error caused by the large discrepancy between beam and slab properties if small values are used. Every effort was made to keep these parameters as close to practical values as possible. The values chosen for the final analysis were

$$A_{BT}/A_{sg} = 0.25$$

$$I_{BT}/I_{sg} = 3.0$$

$$e/t = 3.0$$

where t is the thickness of the slab.

2.3 Finite Element Analysis

The stiffness of each slab/beam assemblage analyzed was determined with the aid of elastic finite element analysis. The computer program that was used in this study was the finite element program FINITE which was developed by Professor Leonard A. Lopez and colleagues [24] at the University of Illinois at Urbana-Champaign. A typical interior panel of a slab was modeled as a plate having both bending and membrane stresses with a rigid column area and a beam in the longitudinal direction (i.e., direction of loading).

The boundary conditions and loading imposed on this typical interior panel were such that the resultant deflected shape was similar to that encountered when the frame is subjected to lateral loading, such as seismic or wind forces. The following sections describe the modeling procedure employed in the analysis.

2.3.1 Mesh

Several meshes were attempted and considerable experimentation with different meshes was employed for determining an efficient, yet accurate, finite element mesh.

The first mesh used consisted of 16 elements in each direction with two different spacings. Ten elements at 0.04 times the half-span, and six at 0.10 times the half-span were used, as shown in Fig. 2.3. This mesh was costly in computation time and was not feasible for the parametric study intended as many runs are required to cover the practical range of the parameters.

In order to reduce computing time, the number of elements were reduced to ten in each direction but with three different spacings which are (Fig. 2.4) four at 0.05 times the half-span, four at 0.10, and two at 0.20. This mesh reduced computation time by about 60 percent, but yielded rotations and deflections about two-thirds of those of the 16 x 16 element mesh, which indicates a condition of being too far away from convergence of the finite element solution.

To seek convergence of the solution, a uniform mesh of 20 elements in each direction was attempted though at a higher computation time. This yielded rotations about twice those for the 16 x 16 element mesh. A 25 x 25 element mesh was also tried and it yielded results virtually identical to those of the 20 x 20 element mesh, which indicates that the solution converges at around the 20 x 20 element mesh.

Since the 20 x 20 element mesh was by no means feasible for the study, a new mesh was attempted that had 25 elements in the longitudinal direction and only two elements in the transverse direction. The width

of the first element is controlled by c_2, the width of the column in the transverse direction. The rotations of this mesh came within about 4 percent of the converged solution provided by the 20 x 20 and 25 x 25 element meshes. The computation time was very fast relative to the original 16 x 16 element mesh, requiring only about 8 percent of its computation time.

This encouraging result led to the final slab mesh employed which had 25 elements longitudinally and 3 elements transversely. The first element had its width controlled by the column size, the next two elements split the remaining transverse span in half. This slab mesh, shown in Fig. 2.5, yielded results that were within 2 percent of the converged 25 x 25 element mesh solution (Fig. 2.6) at about 3 percent of its computation time. This fact made the parametric study of the slab feasible and efficient, yet accurate. This efficiency would not have been possible to achieve with any of the previous meshes attempted. Experimentation with different meshes for finite element analysis, although time-consuming and expensive, usually becomes economical at the end in terms of overall efficiency and feasibility of studies that must change many parameters and perform numerous finite element computations.

The reason why such a mesh (3 x 25 element mesh) provides satisfactory result for this analysis is that it has a large number of elements in the direction of loading (longitudinal) while it has only a few elements in the transverse direction where the rotations are much less. Therefore, the errors introduced by the coarse mesh transversely are small. Although this mesh provides good results for the rotations under consideration and

yields satisfactory overall behavior, one strongly suspects that it does not provide accurate results for local behavior in the transverse direction.

This 3 x 25 element mesh was used for all the analysis, and all results of the study were derived based on the solution using this mesh. Several cases were run, and their results confirmed its overall accuracy of about 2 percent with respect to the more elaborate meshes that were attempted (20 x 20 elements and 25 x 25 elements).

2.3.2 Elements

Two superimposed elements were used for each element in the slab mesh to model all degrees of freedom.

The first element was a Rectangular Plate Bending element having 16 degrees of freedom. It has 4 nodes and is formulated using moderately thick plate theory. The displacement shape for this element is of the third order. Each node has 4 degrees of freedom as shown in Fig. 2.7. Vertical displacement, w, rotation about the x-axis, θ_x, rotation about the y-axis, θ_y, and twist, w_{zy}. The element is completely conforming and rotations are compatible between elements since the element has the warping degree of freedom. Complete formulation and behavior of this element is discussed in Ref. 6.

The generalized stress and strain resultants are defined by the following terms, referring to Fig. 2.8 [24],

$$M_{xx} = D(w_{,xx} + \nu w_{,yy})$$

$$M_{yy} = D(w_{,yy} + \nu w_{,xx})$$

$$M_{xy} = D(1 - \nu)w_{,xy}$$

$$Q_{xx} = D(w_{,xxx} + w_{,xyy})$$

$$Q_{yy} = D(w_{,yyy} + w_{,xxy})$$

$$V_{xx} = D(w_{,xxx} + (2 - \nu)w_{,xyy})$$

$$V_{yy} = D(w_{,yyy} + (2 - \nu)w_{,xxy})$$

where

$$D = \frac{Et^3}{12(1 - \nu^2)}$$

ν = Poisson's ratio

E = Young's modulus of elasticity

t = thickness of the plate

w = vertical displacement (z-axis)

The second superimposed element was a Plane Stress Rectangle having 4 nodes and two degrees of freedom at each node, the x-displacement, u, and the displacement, v, as shown in Fig. 2.9. The generalized stresses and strains for this element are shown in Fig. 2.10.

The beam was modeled using plane frame elements along the y-axis. They were connected with rigid links to the plate elements to represent the eccentricity between the slab and beam neutral axes. The plane frame elements have two nodes with three degrees of freedom at each node: the x-displacement, u, the y-displacement, v, and the rotation about the z-axis, θ_z. These degrees of freedom are with respect to the local axes of the element; however, the element is oriented such that its local x-axis lies along the global y-axis, and its local z-axis lies along the global x-axis.

2.3.3 Constraints

The symmetry of the structure and the antisymmetry of the loading implied that the following boundary conditions be imposed on the panel being analyzed (Fig. 2.11):

(1) The x-displacement, u, and the y-rotation, θ_y, were constrained along the longitudinal column line and longitudinal centerline of the slab.

(2) The vertical displacement, w, was constrained at the transverse column line edge and transverse slab centerline edge.

These constraints enabled the analysis of one quarter of the panel instead of the whole panel, thus greatly reducing computation time.

2.3.4 Loading

The loading for this structure was selected to be a concentrated moment about the global x-axis applied to node 1, which is the column corner of the quarter panel where the three elements, slab, beam and column, meet. This loading models the deflection pattern of this subassemblage when the frame deflects in an antisymmetric manner under lateral forces.

3. RESULTS

Numerous test runs were performed and analyzed before the final finite element runs were selected for purposes of arriving at the results presented. Many of these runs were improved and rerun to obtain the final results presented herein.

3.1 Variation of Parameters

Two approaches were used to obtain the final values. The first approach employed a slab without a beam for the derivation of the flexural effective width coefficients, and the second employed a slab with a beam for determination of the axial effective width coefficients. In each case the variation of the parameters involved was achieved by varying the dimensions of the elements, thus the mesh remained the same for all cases. The rigidity of the column was approximated by increasing the modulus of elasticity of column elements desired to be rigid to 10^5 times that of the remaining elements. This factor was established after some experimentation. It proved to be a good compromise between infinite rigidity which causes round-off error and too small a rigidity that would not yield the desired effect.

3.1.1 Flexural Effective Width

Three main parameters control the flexural effective width coefficient, λ_f:

(1) The aspect ratio of the slab, L_1/L_2. The transverse dimension L_2 was fixed at 100 units of length and L_1 was varied from 50 to 300 units, thus yielding a variation in the aspect ratio

from 0.50 to 3.00. As expected, an increase in the aspect ratio increased the effective width, indicating that a greater fraction of the width of the slab acts like a beam as the slab becomes longer in the loading direction.

(2) The longitudinal relative column dimension, c_1/L_1. The variation of this parameter was accomplished by varying the number of elements being considered rigid from one to six. The parameter c_1/L_1 varied from 0.04 to 0.24 in increments of 0.04, which is the size of one element, encompassing most of the possible practical values. This variation was performed for each of the six aspect ratios considered. The resulting effective widths indicate that as c_1/L_1 increases, the effective width increases though in different magnitudes for different aspect ratios. For small aspect ratios the effect is small, but for large aspect ratios the effect is more pronounced for the smaller values of c_1/L_1; however, the curves level off at smaller values of c_1/L_1 as the aspect ratio increases (Fig. 3.1). Finite element results are listed in Table 3.1, and the derived flexural effective width coefficients are listed in Table 3.5.

(3) The transverse relative column dimension, c_2/L_2. The above two variations were performed with a fixed value of c_2/L_2 of 0.06. This value was chosen because it seemed more representative of what would be encountered in practice. As c_2/L_2 was varied, the flexural effective width coefficient varied linearly. For larger c_2/L_2, λ_f increased in a linear

fashion that was dependent on the aspect ratio of the slab, but seemed to be relatively independent of the value of c_1/L_1 being considered. In general, the variation was slightly higher for lower values of c_1/L_1. Several cases were analyzed, and the relative decoupling between c_2/L_2 and c_1/L_1 was confirmed. The difference noted in λ_f varied in general by less than 1.5 percent as c_1/L_1 was changed from 0.08 to 0.16. Therefore, an average value for c_1/L_1 of 0.12 was chosen to derive the final correction factors used, λ_f/λ_{f_o}, to correct for the transverse column dimension effect. The parameter c_2/L_2 was varied from 0.3 to 0.18. The resulting finite element values shown in Table 3.2 and the calculated correction factors are shown in Table 3.5 and Fig. 3.2.

3.1.2 Axial Effective Width

The same three parameters controlling the flexural effective width were the ones affecting the axial effective width coefficient, λ_a. The same cases used for deriving the flexural coefficient were used for the axial coefficient, with the difference being the addition of a beam.

Numerous test runs with different aspect ratios, relative column dimension, slab thickness, beam eccentricity, beam cross-sectional area, and beam moment of inertia indicated that the axial effective width coefficients are only dependent on L_1/L_2, c_1/L_1, and to a lesser extent c_2/L_2. Therefore, arbitrary practical values for e, A_{BT}, and I_{BT} were chosen for each slab analyzed. They were chosen slighly on the high side to cancel any round-off errors, and because the resultant values

of λ_a will be slightly on the conservative side when used with smaller values.

The same variations in L_1/L_2 and c_1/L_1 as the flexural calculations were used in this study. The resulting finite element stiffnesses are shown in Table 3.3 and the derived λ_{a_o} values are shown in Table 3.7 and Fig. 3.3.

As c_2/L_2 was varied for various values of L_1/L_2, there were small changes in the axial effective width coefficient, λ_a; these changes became less apparent for higher values of L_1/L_2. Analytical results are given in Table 3.4 and the adjusted derived correction factors are shown in Table 3.8 and Fig. 3.4. For L_1/L_2 greater than 1.0, the correction is negligible and is therefore omitted from consideration.

The variation of λ_a with c_1/L_1 was observed to be opposite to that for λ_f. As c_1/L_1 increases, λ_a decreases, and it does so more sharply for larger aspect ratios than for smaller ones. The explanation for this behavior is that as the rigid area becomes larger, there is less remaining span length in the direction of loading; the composite action decreases, thereby reducing the effective area of the slab acting in this manner. Theoretically, the curves should all converge to zero as c_1/L_1 approaches 1.0. The results substantiate this fact. These axial effective width coefficients are independent of the properties of the beam, unless unrealistic values are used, in which case the deviation observed is mainly due to round-off error in the finite element solutions.

3.2 Discussion of Accuracy

It is difficult to specify accuracy of the presented results because, to the best knowledge of the author, no published test data are available

on laterally loaded frames with floor slabs and beams. Other researchers have also confirmed this fact [40]. The proposed method can only be compared to the analytical values obtained from finite element analyses. Therefore, any accuracy referred to in this study is based on such analytical values, and no claim is made on accuracy with respect to experimental testing. Some of the other theoretical studies which are not based on finite element analysis employ empirical distributions of stresses, or are restricted to gravity loading.

The rotations and deflections of the equivalent beam having properties that will give an identical end rotation as the composite slab and beam is very compatible with the deflections obtained by the finite element analysis of the 3 x 25 element mesh and the 20 x 20 element mesh. In fact, the deflections lie between the elaborate mesh and the one being used, which makes the equivalent beam even closer to the converged solution. The deviation is on the order of 1.5 percent.

The results of most of the cases studied in this investigation are tabulated in Tables 3.9 to 3.15, with direct comparison of the resultant composite stiffness using the presented effective width constants with the results of the finite element analysis of those particular slabs. As can be seen from the tables, all values of composite stiffness are within ±2.5 percent of the finite element results. The cases studied present a wide variety of parameters that were varied. While they do not cover every conceivable variation, they show the trends of the variations which led the way to the final results and proposed simplified method of analysis for using the derived effective width coefficients.

The effect of the eccentricity of the beam was to change the equivalent composite stiffness in a quadratic manner as would be expected from Eq. (4). The data from the finite element analysis fit this equation satisfactorily. For zero eccentricity, the composite equivalent stiffness is simply the sum of that of the effective slab and beam without any composite action.

The moment of inertia of the beam was just an additional constant to the composite moment of inertia as long as the area of the beam was not changed. If the area of the beam is changed, then the position of the composite neutral axis changes as well as the composite action between the slab and the beam. The effect of changing the thickness of the slab is more involved, especially as the gross area and moment of inertia of the slab are changed simultaneously. The position of the composite neutral axis is changed, composite action is changed, and the slab effective moment of inertia also is changed.

3.3 Proposed Method for Using the Effective Width Coefficients

The recommended procedure for calculating the composite stiffness of the slab and beam using the derived results is the following:

(1) Enter Fig. 3.1 with the desired value of the longitudinal relative column size, c_1/L_1. For the appropriate curve for the aspect ratio of the slab being considered, L_1/L_2, read the value of the flexural effective width coefficients, λ_{f_o}. Linear interpolation may be used for values that are not plotted.

(2) Enter Fig. 3.2 with the desired value of the transverse

relative column size, c_2/L_2. For the appropriate curve for the aspect ratio of the slab under consideration, read the correction factor for λ_f. Calculate λ_f, where

$$\lambda_f = \lambda_{f_o} \times \text{(flexural correction factor)}$$

(3) Enter Fig. 3.3 with the value of the longitudinal relative column size. For the appropriate curve for the aspect ratio under consideration, read the value of the axial effective width coefficient, λ_{a_o}.

(4) From Fig. 3.4 read the correction factor for the axial effective width coefficient for the appropriate aspect ratio and transverse relative column size. Calculate λ_a, where

$$\lambda_a = \lambda_{a_o} \times \text{(axial correction factor)}$$

(5) Determine the position of the composite neutral axis from

$$y = A_{BT}e/(A_{BT} + \lambda_a A_{sg})$$

(6) Calculate the equivalent moment of inertia of the composite section referred to the modulus of elasticity of the slab from

$$I_{eq} = \lambda_a A_{sg} + \lambda_f I_{sg} + I_{BT}$$

This calculated composite moment of inertia does not include the rigidity effect of the finite column dimension. Therefore, when the equivalent beam is analyzed as part of a frame, rigid links must be imposed at the ends of the equivalent beams to account for this effect.

If the equivalent beam is to be analyzed without this rigidity imposed, then I_{eq} has to be corrected to include this rigidity.

The corrected value, I'_{eq}, should then be used in the frame, where

$$I'_{eq} = I_{eq}/(1 - c_1/L_1)^3$$

Use of the corrected moment of inertia in such a manner will yield accurate results for the end rotations of the equivalent beam, but may not be as accurate for evaluating the deflections of the slab/beam. Also, the equivalent moment of inertia may be larger than that obtained by considering the whole width of the slab as an equivalent beam. This situation arises because the additional stiffness offered by the finite dimension of the column is essentially added to the stiffness of the slab. Such a case arises if the aspect ratio of the slab is large or the relative dimension of the column is large. However, the nodal effective stiffness of the slab will be correct. If only the nodal stiffness of the equivalent beam is of primary concern, then the equivalent moment of inertia may be used in any of the two forms described.

3.4 Remarks on Applicability

The results presented in this chapter were derived from the analysis of typical interior panels, and technically the results are applicable only in such cases. However, a few cases of end panels were studied, and their results showed that the proposed method can be applied satisfactorily. The error involved in such cases was observed to be on the order of 10 percent.

Also, a few cases were analyzed where a transverse beam was present at the column line which was about half the size of the

longitudinal beam. The results obtained were very close to those without the torsional beam. One reason for this observation possibly is that the boundary conditions do not allow for large relative torsional rotation of that beam.

4. EXAMPLE APPLICATIONS

There are several possible applications of composite slab and beam behavior in structural analysis and design. The proposed method was derived based on laterally loaded frames and was mainly intended for application in seismic design. However, it may be applied for wind loading and any other loading pattern of a frame that produces the anti-symmetric deflection shape described previously.

The proposed effective width factors may be applied to steel as well as concrete frames. Although derived for a slab of uniform thickness, the method can apply to slabs that do not have a uniform thickness, such as ribbed slabs or steel joist floor systems provided the gross area and moment of inertia of the slab is computed, and the position of the neutral axis of the slab is determined. A nonuniform slab will make the computation of composite stiffness more involved, but the theory should still apply.

For the design of the composite member, any suitable method may be used, depending on the situation at hand. Ultimate design, as per ACI Code [3], or working stress design may be employed. The effect of cracking also may be considered by using a cracked moment of inertia for the slab as recommended by the ACI Code. The designing process always will follow the preliminary analysis; therefore, once the effective widths are determined, the engineer has many choices for design using an appropriate procedure. While the design procedure for the structural members of a frame is certainly important, it is not the purpose of this study to suggest methods for member design. However,

it is the main purpose of this investigation to recommend modification of member properties as a tool for analyzing frames subject to lateral forces.

The examples presented in this chapter are for the purpose of illustrating the use of the proposed method and some of its effects in analyzing low-rise steel frames for seismic loading. The method of analysis was chosen for simplicity and does not necessarily limit the use of the study to the type of frame or method of analysis discussed.

4.1 Composite Member Properties of a Slab

For determination of composite properties of a floor system, a square interior panel of a concrete slab 5 inches thick having a span of 20 feet is selected. The beam is a W24x68 steel section, and the column is W14x68 steel section. The concrete compressive strength used in this example is 3500 psi.

The dimensions of the steel column are [5]:

$$c_1 = 14.06 \text{ inches}$$

$$c_2 = 10.04 \text{ inches}$$

which gives

$$c_1/L_1 = 0.059$$

$$c_2/L_2 = 0.042$$

The flexural effective width ratio is determined from Fig. 3.1 for the aspect ratio, $L_1/L_2 = 1.0$,

$$\lambda_{f_o} = 0.54$$

The correction factor for the transverse relative column size is determined from Fig. 3.2,

$$\lambda_f/\lambda_{f_o} = 0.98$$

Therefore,

$$\lambda_f = 0.54 \times 0.98 = 0.53$$

Similarly, the axial effective width coefficient is determined from Fig. 3.3,

$$\lambda_{a_o} = 0.34$$

And the correction factor for c_2/L_2 is determined from Fig. 3.4,

$$\lambda_a/\lambda_{a_o} = 1.01$$

Therefore,

$$\lambda_a = 0.34 \times 1.01 = 0.34$$

The properties of the beam as obtained from the 7th edition of the AISC Manual [5] are the following:

$$A_B = 20.0 \text{ in.}^2$$

$$I_B = 1820 \text{ in.}^4$$

$$d = 23.71 \text{ in.}$$

where d is the depth of the steel beam.

Since the slab and beam are of two different materials, their properties must be transformed to the same modulus of elasticity. The modulus of elasticity of concrete may be taken as suggested by the ACI Code [3],

$$E = 57000\sqrt{f'_c}$$

which gives the modulus of elasticity of the slab, E_s,

$$E_s = 3370 \text{ ksi}$$

The modulus of elasticity of the steel is taken as 29,000 ksi giving a modular ratio, n, of

$$n = \frac{29000}{3370} = 8.60$$

Therefore the transformed properties of the beam become

$$A_{BT} = nA_B = 8.60 \times 20.0 = 172.0 \text{ in.}^2$$

$$I_{BT} = nI_B = 8.60 \times 1820 = 15650 \text{ in.}^4$$

The gross area and moment of inertia of the slab are calculated as follows:

$$A_{sg} = L_2 t = (20 \times 12) \times 5 = 1200 \text{ in.}^2$$

$$I_{sg} = L_2 t^3/12 = 1280 \text{ in.}^4$$

The eccentricity of the beam's neutral axis below that of the slab is given by

$$e = (d + t)/2 = (23.71 + 5)/2 = 14.36 \text{ in.}$$

The position of the neutral axis of the composite section can now be calculated,

$$y = \frac{A_{BT}e}{A_{BT} + \lambda_a A_{sg}} = \frac{172.0 \times 14.36}{172.0 + (0.34 \times 1200)} = 4.23 \text{ in.}$$

Finally, the equivalent composite moment of inertia can be computed,

$$I_{eq} = \lambda_a A_{sg} ey + \lambda_f I_{sg} + I_{BT}$$

$$= (0.34 \times 1200 \times 14.36 \times 4.23) + (0.53 \times 1280) + 15650$$

$$= 41300 \text{ in.}^4$$

and the equivalent composite area is

$$A_{eq} = \lambda_a A_{sg} + A_{BT} = (0.34 \times 1200) + 172.0$$

$$= 583.6 \text{ in.}^2$$

These properties are equivalent concrete properties of the composite section since it is referred to the modulus of elasticity of the slab. If it is desired to reference them to the beam's modulus of elasticity, they should be divided by the modular ratio, n,

$$(I_{eq})_{steel} = 41300/8.60 = 4800 \text{ in.}^4$$

$$(A_{eq})_{steel} = 583.6/8.60 = 67.9 \text{ in.}^2$$

It is interesting to compare these properties to the ones obtained if the whole width of slab is assumed to be effective in composite action, and to the properties of the beam by itself,

$$(I_{eq})_{full\ width} = 5570 \text{ in.}^4 \qquad I_B = 1820 \text{ in.}^4$$

$$(A_{eq})_{full\ width} = 159.5 \text{ in.}^2 \qquad A_B = 20.0 \text{ in.}^2$$

As expected, the properties based on the full width are considerably larger than the values using the effective width.

The computed effective composite properties do not include the effect of column rigidity, If this effect is desired to be included, the computed values must be divided by the quantity $(1 - c_1/L_1)^3$.

The resulting properties become

$$I'_{eq} = 4800/(1 - 0.059)^3 = 5760 \text{ in.}^4$$

$$A'_{eq} = 67.9/(1 - 0.059)^3 = 81.5 \text{ in.}^2$$

It is a debatable matter whether or not this rigidity effect should be considered. The behavior of the column area is somewhere between infinite rigidity and zero rigidity. This contact area of slab is stiffer than the rest of the slab, but not necessarily fully rigid. Since conventional frame analysis neglects this rigidity effect, it may be more desirable not to correct the resultant equivalent composite beam properties for this extra rigidity.

4.2 Seismic Analysis of a Frame

To illustrate the application of the proposed method in seismic design of buildings, a three-story moment-resisting steel frame is chosen for analysis. A smoothed elastic response spectrum [32] is used as the earthquake input. Modal analysis is performed, and the results are compared to those obtained by analyzing the frame with the slab stiffness neglected.

The three-story frame selected is a two-bay frame with a span of 22 feet each as shown in Fig. 4.1. The columns used are all W14x127 and the beams are W21x68, all of them made of A36 steel. The floor systems selected are all uniform six-inch reinforced concrete with a compressive strength of 3500 psi. The transverse span selected is 20 feet.

4.2.1 Gravity Loads

The dead load considered for this frame was computed as follows:

6" Concrete slab	72 psf
Steel members	8 psf
Partitions	20 psf
Total DL	100 psf

The live load was taken as 40 psf, a common loading for residential buildings. Although the roof usually carries less live load than the rest of the floors, it was taken to be the same in this example in order to facilitate the computations.

4.2.2 Equivalent Composite Beam Properties

The dimensions of the W14x127 steel column are obtained from the 1973 AISC Manual [5],

$$c_1 = 14.62 \text{ in.}$$

$$c_2 = 14.69 \text{ in.}$$

which gives the relative column size as

$$c_1/L_1 = \frac{14.62}{22 \times 12} = 0.055$$

$$c_2/L_2 = \frac{14.69}{20 \times 12} = 0.061$$

The aspect ratio of the slab is

$$L_1/L_2 = 22/20 = 1.1$$

The flexural and axial effective width coefficients obtained from Figs. 3.1 through 3.4 are

$$\lambda_f = 0.567$$

$$\lambda_a = 0.374$$

The properties of the beam as obtained from the 1973 AISC Manual are

$$I_B = 1480 \text{ in.}^4$$

$$A_B = 20.0 \text{ in.}^2$$

$$d = 21.13 \text{ in.}$$

If the properties of the slab and beam are transformed to the same modulus of elasticity using the modular ratio (n = 8.6), the resultant equivalent composite properties referenced to the modulus of elasticity of the beam (E = 29000 ksi) are

$$I_{eq} = 4554 \text{ in.}^4$$

$$A_{eq} = 82.6 \text{ in.}^2$$

For consistency of comparison with the frame analysis which neglects the slab, the above properties were used without modification for the column rigidity effect. The analysis of the frame neglecting the slab does not take this effect into consideration, so proper comparison should not include this factor. Otherwise, the results may be misleading.

4.2.3 Modal Analysis

The stiffness matrix for lateral forces was determined by applying unit horizontal displacements at each level, one at a time, while restraining the remaining horizontal degrees of freedom, and calculating the resulting horizontal forces. This analysis was performed with the

aid of finite element analysis. The rotations and vertical displacements of the joints were not restrained. Their effect is included in the condensed stiffness matrix for lateral forces. The numbering of the degrees of freedom is as shown in Fig. 4.2.

The resulting stiffness matrix for the frame neglecting the slab was calculated as follows:

$$[K] = \begin{bmatrix} 896 & -505 & 103 \\ -505 & 710 & -331 \\ 103 & -331 & 245 \end{bmatrix} \text{ k/in.}$$

The stiffness matrix for the frame, including the slab effective stiffness, was calculated as follows:

$$[K] = \begin{bmatrix} 953 & -515 & 70 \\ -515 & 854 & -417 \\ 70 & -417 & 353 \end{bmatrix} \text{ k/in.}$$

As expected, the lateral stiffness of the frame, including the stiffness of the slab is greater than that when the slab stiffness is neglected.

The mass matrix for the frame was taken as a lumped mass matrix, and no mass is attributed to the rotational degrees of freedom at the nodes where the masses are lumped. The load used to compute the mass per floor was the dead load plus 25 percent of the live load. This load leads to a weight per floor, W, of

$$W = (100 + (0.25 \times 40)) \times 44 \times 20 = 96.8 \text{ k}$$

and leads to a floor mass of

$$m = \frac{W}{g} = \frac{96800 \text{ lb}}{386 \text{ in./sec}^2} = 251 \text{ lb-sec}^2/\text{in.}$$

and the lumped mass matrix is

$$[m] = 251 \begin{bmatrix} 1 & 0 & 0 \\ 0 & 1 & 0 \\ 0 & 0 & 1 \end{bmatrix} \text{lb-sec}^2/\text{in.}$$

In order to calculate the natural frequencies of vibration, the characteristic equation has to be solved,

$$|[K] - \omega^2[m]| = 0$$

The characteristic equation is a cubic function in ω^2. The solution to this cubic equation provides the square of the natural circular frequencies, from which the frequencies may be calculated by

$$f = \frac{\omega}{2\pi}$$

For the frame with the slab neglected, the natural frequencies are

$$f_1 = 1.95 \text{ Hz}$$

$$f_2 = 6.52 \text{ Hz}$$

$$f_3 = 11.85 \text{ Hz}$$

If the effective stiffness is considered, the natural frequencies of vibration are increased to the following values:

$$f_1 = 2.50 \text{ Hz}$$

$$f_2 = 7.64 \text{ Hz}$$

$$f_3 = 12.39 \text{ Hz}$$

The mode shapes can be computed from the characteristic matrix by substituting into the characteristic matrix one frequency at a time. The mode shape for that frequency (scaled to an arbitrary constant) is the vector obtained by taking any row of the matrix of cofactors of the characteristic matrix. In this example, the mode shapes are scaled by the component of the first degree of freedom. The resulting mode shapes, $\{\phi_n\}$, for each vibrating frequency, without considering the slab stiffness, are as follows:

$$\{\phi_1\} = \begin{Bmatrix} 1.000 \\ 2.368 \\ 3.284 \end{Bmatrix} \qquad \{\phi_2\} = \begin{Bmatrix} 1.000 \\ 0.799 \\ -0.919 \end{Bmatrix} \qquad \{\phi_3\} = \begin{Bmatrix} 1.000 \\ -0.784 \\ 0.303 \end{Bmatrix}$$

while for the frame with the slab considered, the mode shapes are as follows:

$$\{\phi_1\} = \begin{Bmatrix} 1.000 \\ 2.110 \\ 2.775 \end{Bmatrix} \qquad \{\phi_2\} = \begin{Bmatrix} 1.000 \\ 0.616 \\ -0.828 \end{Bmatrix} \qquad \{\phi_3\} = \begin{Bmatrix} 1.000 \\ -1.042 \\ 0.432 \end{Bmatrix}$$

The participation factor for each mode, α_n, may now be calculated. The participation factor for mode n is defined as

$$\alpha_n = \frac{\{\phi_n\}^T[m]\{1\}}{\{\phi_n\}^T[m]\{\phi_n\}}$$

The calculated participation factors for the frame neglecting the slab are

$$\alpha_1 = 0.383 \qquad \alpha_2 = 0.354 \qquad \alpha_3 = 0.305$$

while those for the frame considering the slab are

$$\alpha_1 = 0.447 \qquad \alpha_2 = 0.381 \qquad \alpha_3 = 0.171$$

A smoothed response spectrum as suggested in Ref. 32 was used with a base ground acceleration, a_g, of 0.15 g. The ground motions were calculated for competent soil with the recommended value of v/a ratio of 36 in./sec/g and an ad/v^2 equal to 6.0. The amplification factors were computed for 5 percent damping and a cumulative probability of 84.1 percent, which is the median plus one standard deviation. The resulting amplification factors for acceleration, A, velocity, V, and displacement, D, are

$$A = 2.71$$

$$V = 2.30$$

$$D = 2.01$$

The design elastic response spectrum is then drawn as suggested in Ref. 32 and is shown in Fig. 4.3. The resulting spectral acceleration, S_{an}, for the three modes of vibration can now be read directly from this response spectrum for the three natural frequencies of vibration. For the frame without the slab considered, the spectral accelerations for the three modes are

$$S_a = \begin{Bmatrix} 0.41 \\ 0.41 \\ 0.32 \end{Bmatrix} g$$

while the spectral accelerations for the frame with the effective slab considered are

$$S_a = \begin{Bmatrix} 0.41 \\ 0.41 \\ 0.30 \end{Bmatrix} g$$

The story forces, f_{sn}, may now be calculated for each mode of vibration using the participation factor, the mode shape, and the spectral acceleration for that mode [11, 31, 38]

$$\{f_{sn}\} = [m]\alpha_n\{\phi_n\}S_{an}$$

The resulting forces for the frame without consideration of the slab stiffness for the three natural modes of vibration are

$$f_{s_1} = \begin{Bmatrix} 15.2 \\ 35.9 \\ 49.9 \end{Bmatrix} \text{kips} \qquad f_{s_2} = \begin{Bmatrix} 14.1 \\ 11.3 \\ -12.9 \end{Bmatrix} \text{kips} \qquad f_{s_3} = \begin{Bmatrix} 9.5 \\ -7.4 \\ 2.9 \end{Bmatrix} \text{kips}$$

The lateral story forces for the frame, including the slab stiffness, are

$$f_{s_1} = \begin{Bmatrix} 17.2 \\ 36.4 \\ 48.0 \end{Bmatrix} \text{kips} \qquad f_{s_2} = \begin{Bmatrix} 14.7 \\ 9.1 \\ -12.2 \end{Bmatrix} \text{kips} \qquad f_{s_3} = \begin{Bmatrix} 4.9 \\ -5.1 \\ 2.1 \end{Bmatrix} \text{kips}$$

These modal story forces are the maximum amplitude of the forces when the system is vibrating in that mode of vibration. The total response is obtained through superposition of the three modes. However, this superposition is in the time domain. The maximum total response cannot be obtained, in general, by merely adding the modal maxima. The modal maxima generally do not occur at the same time. Therefore, although adding the modal response maxima provides an upper limit to

the total response, it is in general an overestimation of the maximum response likely to be encountered.

There are several proposed methods to obtain a reasonable estimate of the maximum response from the spectral values. The simplest method is to take the square root of the sum of the squares of the modal maximum values as the most probable estimate, or

$$f_{s,max} = \sum_{n=1}^{3} \left[(f_{sn})^2 \right]^{1/2}$$

The maximum values of the story forces computed by this method for the frame neglecting the slab are

$$f_{s,max} = \begin{Bmatrix} 22.8 \\ 38.4 \\ 51.6 \end{Bmatrix} \text{ kips}$$

and the maximum computed forces for the frame with the effective slab considered are

$$f_{s,max} = \begin{Bmatrix} 23.1 \\ 37.9 \\ 49.6 \end{Bmatrix} \text{ kips}$$

Now the base shear for each mode can be computed by summing forces at all the story levels, and the maximum value may be computed by square root of the sum of the squares method. The base shears, V_{bn}, neglecting the slab are

$V_{b_1} = 101.0$ kips $\quad V_{b_2} = 12.5$ kips $\quad V_{b_3} = 5.0$ kips

$V_{b,max} = 101.9$ kips

If the slab is considered, the base shear values become

V_{b_1} = 101.6 kips $\quad$ V_{b_2} = 11.6 kips $\quad$ V_{b_3} = 1.9 kips

$V_{b,max}$ = 102.3 kips

The frame can now be analyzed in a quasi-static manner by imposing the computed modal story forces on the frame, one mode at a time, and computing the resulting maximum member forces and moments for combination of loadings by taking the square root of the sum of the squares of the modal values. The loadings considered were DL + LL and DL + 0.25LL + Earthquake Load. The analysis of the frame was performed by finite element analysis. The distribution of the lateral forces at each level was such that the interior joints took twice the lateral force imposed on the exterior joints. This distribution was employed because the interior joints have twice the lumped mass of the exterior joints; therefore, they experience twice the inertial forces of the outer joints. As expected, maximum member forces and moments occurred for the second type of loading, the critical members being the first-story beams and the interior first-story column.

When the slab was not considered, these maximum member forces were

$$P_{col.} = 151 \text{ kips}$$

$$M_{col.} = 302 \text{ k-ft}$$

$$M_{beam} = 325 \text{ k-ft}$$

When the slab was considered, the maximum member forces became

$$P_{col.} = 155 \text{ kips}$$

$$M_{col.} = 257 \text{ k-ft}$$

$$M_{beam} = 353 \text{ k-ft}$$

The moment on the critical column is considerably reduced because the stiffer equivalent beam carries a larger share of the applied moment. Although the moment on the critical beam has become larger, the composite beam now has a higher moment capacity than the steel beam by itself, as noted later.

For this example, the capacity of the column may be computed for the combination of axial force and moment. The modified formula (1.6-1b) of the AISC specifications [5] may be used to compute the required tabular load for the above loading, which gives for the case neglecting the slab

$$P + P' = 680 \text{ kips}$$

When the slab effective stiffness is considered, the required tabular load for the column becomes

$$P + P' = 602 \text{ kips}$$

The tabulated load for the W14x127 column is 721 kips [5]. It can be seen that without considering the slab stiffness, the analysis indicates that the column is highly stressed and is approaching its capacity limit. However, taking the effective stiffness of the slab into consideration suggests that the column is not as highly stressed, and may be slightly overdesigned. A column one or two sizes smaller (W14x119 or W14x111) may be used instead.

Similarly, the resisting moment capacity of the W21x68 beam by itself is 280 k-ft, which is less than the bending moment acting on it. If the capacity of the composite section is calculated using the formula $\sigma = Mc/I$, the resisting moment of the composite section becomes 431 k-ft, exceeding the applied moment on the section. Again, without consideration of the slab stiffness, the results would indicate that a larger beam must be chosen when in fact the section is adequate if it is considered to act compositely with the slab.

It is interesting to note that if the frame with the composite slab and beam was analyzed with the computed modal lateral forces using moment distribution instead of finite element analysis, the resulting maximum moments on the critical members are almost identical. The resulting moments are

$$M_{col.} = 256 \text{ k-ft}$$

$$M_{beam} = 344 \text{ k-ft}$$

The calculated axial load on the first-story interior column in this case is 161 kips instead of 155 kips obtained by finite element analysis.

This example illustrates that for low-rise buildings, in general, the floor system contributes a substantial added resistance against dynamic loads, which increases the reserve capacity of the building in resisting lateral loads.

4.3 Concluding Remarks on Seismic Analysis

The preceding example illustrated some of the effects of the proposed method on the seismic analysis of a low-rise steel frame.

The natural frequencies of this low-rise frame were in the range where the smoothed elastic response spectrum had a constant spectral acceleration for the first two modes. Consequently, when the slab was considered, the shift in the natural frequencies of vibration caused little change in the spectral accelerations. The mode shapes changed slightly and the resulting story forces were close to those obtained neglecting the slab; however, in general, the forces on the higher stories were less. The distribution of member forces changed considerably. The bending moments acting on the columns were reduced because the stiffer composite beams carry more moment. The distribution of ductility demand also may change because of the change in the distribution of moments on the sections, and because of the increase in the resisting moment capacity of the composite beams. In general, for low-rise buildings, the slab usually provides an additional margin of safety for the frame in resisting lateral seismic forces. Neglecting the slab in the design of the frame will usually result in a design that has a higher resistance against seismic loading than anticipated by the designer.

REFERENCES

1. Aalami, B., "Moment-Rotation Relation between Column and Slab," Journal of the American Concrete Institute, Vol. 69, No. 5, May 1972, pp. 263-269.

2. Abdel-Sayed, G., Temple, M. C., and Madugula, M. K. S., "Response of Composite Slabs to Dynamic Loads," Canadian Journal of Civil Engineering, Vol. 1, No. 1, Sep. 1974, pp. 62-70.

3. ACI Committee 318, "Building Code Requirement for Reinforced Concrete (ACI 318-77)," American Concrete Institute, Detroit, Mich., 1977.

4. ACI Committee 318, "Commentary of Building Code Requirements for Reinforced Concrete (ACI 318-77)," American Concrete Institute, Detroit, Mich., 1977.

5. AISC, "Manual of Steel Construction," 7th ed., American Institute of Steel Construction, Inc., New York, N.Y., 1973.

6. Bogner, F. K., Fox, R. C., and Schmit, L. A., Jr., "The Generation of Interelement Compatible Stiffness and Mass Matrices by the Use of Interpolation Formulas," Proceedings of the First Conference on Matrix Methods in Structural Mechanics, 26-28 Oct. 1965, Wright-Patterson Air Force Base, Ohio.

7. Bathe, K. J., "ADINA, A Finite Element Program for Automatic Dynamic Incremental Nonlinear Analysis," Rep. 82448-1, Massachusetts Institute of Technology, Cambridge, Mass., May 1976.

8. Bell, J. C., "A Complete Analysis of Reinforced Concrete Slabs and Shells," Thesis presented to the University of Canterbury, at Christchurch, New Zealand, in 1970, in partial fulfillment of the requirements for the degree of Doctor of Philosophy.

9. Carpenter, J. E., "Flexural Characteristics of Flat Plate Floors in Buildings Subjected to Lateral Loads," Thesis presented to Purdue University, at Lafayette, Indiana, in 1965, in partial fulfillment of the requirements for the degree of Doctor of Philosophy.

10. Caughey, R. A., "Composite Beams of Concrete and Structural Steel," Proceedings, 41st Annual Meeting, Iowa Engineering Society, 1929.

11. Clough, R. W., and Penzien, J., Dynamics of Structures, McGraw-Hill, Inc., 1975.

12. Corely, W. G., Sozen, M. A., and Siess, C. P., "The Equivalent-Frame Analysis for Reinforced Concrete Slabs," Civil Engineering Studies, SRS No. 218, University of Illinois, Urbana, June 1961.

13. Corely, W. G., and Jirsa, J. O., "Equivalent Frame Analysis for Slab Design," Journal of the American Concrete Institute, Vol. 67, No. 11, Nov. 1970.

14. Elias, Z. M., and Georgiadis, C., "Flat Slab Analysis Using Equivalent Beams," Journal of the American Concrete Institute, Oct. 1979, p. 1063.

15. Hawkins, N. M., "Shear and Moment Transfer between Concrete Flat Plates and Columns," Progress Report on NSF Grant No. GK-16375, Department of Civil Engineering, University of Washington, Seattle, Wash., Dec. 1971.

16. Hawkins, N. M., Mitchell, D., and Sheu, M. S., "Reversed Cyclic Loading Behavior of Reinforced Concrete Slab-Column Connection," Proceedings of the U.S. National Conference on Earthquake Engineering, 1975, pp. 306-315.

17. Humar, J. L., "Composite Beams under Cyclic Loading," Journal of the Structural Division, ASCE, Vol. 105, No. ST10, Oct. 1979, pp. 1949-1965.

18. Jirsa, J. O., Sozen, M. A., and Siess, C. P., "The Effect of Pattern Loadings on Reinforced Concrete Slabs," Civil Engineering Studies, SRS No. 269, University of Illinois, Urbana, July 1963.

19. Jofriet, J. C., and McNiece, G. M., "Finite Element Analysis of Reinforced Concrete Slabs," Journal of the Structural Division, ASCE, Vol. 97, No. ST3, Mar. 1971.

20. Von Karman, T., "Die Mittragende Breitte," Collected Works of Theodore von Karman, Vol. 11, p. 176.

21. Khan, F. R., and Sbarounis, J. A., "Interaction of Shear Walls and Frames," Journal of the Structural Division, ASCE, Vol. 90, No. ST3, June 1964, pp. 285-335.

22. Lee, J. A. N., "Effective Widths of Tee-Beams," Structural Engineer, London, Jan. 1962.

23. Lin, C. S., "Nonlinear Analysis of Reinforced Concrete Slabs and Shells," Thesis presented to the University of California, Berkeley, California, in 1972, in partial fulfillment of the requirements for the degree of Doctor of Philosophy.

24. Lopez, L. A., et al., "Polo-Finite, A Structural Mechanics System for Linear and Nonlinear Analysis," Technical Report, Civil Engineering Systems Laboratory, University of Illinois, Urbana, Illinois, and Department of Civil Engineering and the Academic Computer Center, University of Kansas, Lawrence, Kansas, 1979.

25. Ma, S. Y. M., Bertero, V. V., and Popov, E. P., "Experimental and Analytical Studies on the Hysteretic Behavior of Reinforced Concrete Rectangular and T-Beams," Earthquake Engineering Research Center, EERC 76-2, University of California, Berkeley, May 1976.

26. MacKay, H. M., Gillespie, P., and Leluau, C., "Report on the Strength of Steel I-Beams Haunched with Concrete," Engineering Journal, Engineering Institute of Canada, Vol. 6, No. 8, 1923, pp. 365-369.

27. Mahin, S. A., et al., "Response of the Olive View Hospital Main Building During the San Fernando Earthquake," Earthquake Engineering Research Center, EERC 76-22, University of California, Berkeley, Oct. 1976.

28. Malik, L. E., and Bertero, V. V., "Contribution of a Floor System to the Dynamic Characteristics of Reinforced Concrete Buildings," Earthquake Engineering Research Center, EERC 76-30, University of California, Berkeley, Dec. 1976.

29. Mondkar, D. P., and Powell, G. H., "ANSR-I General Purpose Computer Program for Analysis of Non-Linear Structure Response," Earthquake Engineering Research Center, EERC 75-37, University of California, Berkeley, 1975.

30. "NASTRAN, the NASA Structural Analysis Program," McNeal Schwendler Corporation, 1977.

31. Newmark, N. M., and Hall, W. J., Fundamentals of Earthquake Engineering, Prentice-Hall, Inc., Englewood Cliffs, N.J., 1971.

32. Newmark, N. M., and Hall, W. J., "Development of Criteria for Seismic Review of Selected Nuclear Power Plants," U.S. Nuclear Regulatory Commission, Report NUREG-CR 0098, 1978.

33. Parma, D., "Equivalent Frame Stiffness Solution for Lateral and Gravity Loads," Paper presented at the ACI Fall Convention, Mexico City, Mexico, Oct. 1976.

34. Pecknold, D. A. W., "Slab Effective Width for Equivalent Frame Analysis," Journal of the American Concrete Institute, Vol. 72, No. 4, April 1975.

35. Reissner, E., "Uber die Berechnung von Plattenbolkan," Der Stahlbau, Dec. 1954.

36. Rotter, J. M., and Ansourian, P., "Cross-Section Behavior and Ductility on Composite Beams," Research Report No. R329, School of Civil Engineering, The University of Sidney, Sidney, Australia, Sep. 1978.

37. Schuster, R. M., "Composite Steel-Deck Concrete Floor Systems," Journal of the Structural Division, ASCE, Vol. 102, No. ST5, May 1976.

38. Timoshenko, S., Young, D. H., and Weaver, W., Jr., Vibration Problems in Engineering, 4th ed., John Wiley & Sons, New York, N.Y., 1974.

39. Vanderbilt, M. D., "Equivalent Frame Analysis for Lateral Loads," Journal of the Structural Division, ASCE, Vol. 105, No. ST10, Oct. 1979, pp. 1981-1997.

40. Viest, I. M., "Review of Research on Composite Steel-Concrete Beams," Journal of the Structural Division, ASCE, Vol. 86, No. ST6, June 1960, pp. 1-21.

41. Wai, K. T., and Adel, A. M., "Effective Width of Coupling Slabs in Shear Wall Buildings," Journal of the Structural Division, ASCE, Vol. 103, No. ST3, Mar. 1977.

42. Youssef, A. A.-R., et al., "Inelastic Analysis of Plates and Slabs Using Finite Elements," Structural Concrete Series, No. 71-1, McGill University, Montreal, Mar. 1971.

43. Youssef, A. A.-R., "Inelastic Bending of Rectangular Plates and Prestressed Concrete Slabs," Thesis presented to McGill University, Montreal, Canada, in 1971, in partial fulfillment of the requirements for the degree of M. Eng.

Table 3.1 Flat Slab Stiffness, $M/E_s\theta_o$, for Varying Aspect Ratio, L_1/L_2, and Longitudinal Relative Column Size, c_1/L_1

$L_2 = 100.0$ $c_2 = 6.0$ $t = 4.0$

	c_1/L_1					
L_1/L_2	0.04	0.08	0.12	0.16	0.20	0.24
0.50	12.31	14.56	17.10	20.00	23.34	27.24
0.75	10.42	12.58	14.96	17.62	20.67	24.18
1.00	9.39	11.48	13.73	16.23	19.04	22.26
1.50	7.99	9.84	11.76	13.84	16.15	18.81
2.00	6.92	8.47	10.03	11.70	13.56	15.72
3.00	5.37	6.43	7.47	8.59	9.91	11.54

Note: Refer to Sec. 1.4 for consistency of units.

Table 3.2 Flat Slab Stiffness, $M/E_s\theta_o$, for Varying Aspect Ratio, L_1/L_2, and Transverse Relative Column Size, c_2/L_2

$L_2 = 100.0$ $\quad c_1/L_1 = 0.12$ $\quad t = 4.0$

	c_2/L_2			
L_1/L_2	0.03	0.06	0.12	0.18
0.50	15.68	17.10	19.98	22.87
0.75	14.01	14.96	16.85	18.74
1.00	13.04	13.73	15.09	16.41
1.50	11.38	11.76	12.49	13.18
2.00	9.80	10.03	10.44	10.83
3.00	7.33	7.47	7.63	7.78

Note: Refer to Sec. 1.4 for consistency of units.

Table 3.3 Composite Stiffness, $M/E_s\theta_o$, for Varying Aspect Ratio, L_1/L_2, and Longitudinal Relative Column Size, c_1/L_1

$L_2 = 100.0$ $t = 4.0$ $A_{BT} = 100.0$

$c_2 = 6.0$ $e = 12.0$ $I_{BT} = 1600.0$

	c_1/L_1					
L_1/L_2	0.04	0.08	0.12	0.16	0.20	0.24
0.50	541.05	605.94	681.77	771.23	877.14	1003.19
0.75	418.26	468.24	526.68	595.63	677.73	775.95
1.00	348.33	389.67	438.06	495.02	562.87	644.08
1.50	262.24	294.76	331.54	374.87	426.33	488.01
2.00	209.98	235.39	265.14	300.28	342.06	392.44
3.00	147.45	165.53	186.80	212.08	242.50	279.34

Note: Refer to Sec. 1.4 for consistency of units.

Table 3.4 Composite Stiffness, $M/E_s\theta_o$, for Varying Aspect Ratio, L_1/L_2, and Transverse Relative Column Size, c_2/L_2

$L_2 = 100.0$ $t = 4.0$ $A_{BT} = 100.0$
$c_1/L_1 = 0.12$ $e = 12.0$ $I_{BT} = 1600.0$

	c_2/L_2			
L_1/L_2	0.03	0.06	0.12	0.18
0.50	698.69	681.77	670.45	674.99
0.75	531.73	526.68	524.01	526.22
1.00	439.72	438.06	437.44	439.00
1.50	331.74	331.54	331.89	332.83
2.00	265.02	265.14	265.72	266.43
3.00	186.56	186.80	187.37	187.90

Note: Refer to Sec. 1.4 for consistency of units.

Table 3.5 Flexural Effective Width Coefficients, λ_{f_o}, for Varying Aspect Ratio and Longitudinal Relative Column Size

	c_1/L_1					
L_1/L_2	0.04	0.08	0.12	0.16	0.20	0.24
0.50	0.340	0.354	0.364	0.370	0.373	0.374
0.75	0.432	0.459	0.478	0.490	0.496	0.498
1.00	0.519	0.559	0.585	0.601	0.609	0.611
1.50	0.663	0.719	0.752	0.769	0.775	0.775
2.00	0.765	0.825	0.854	0.867	0.868	0.868
3.00	0.890	0.939	0.954	0.955	0.955	0.955

Note: $c_2/L_2 = 0.06$ for all values. For c_2/L_2 different from 0.06, above values must be corrected using the appropriate correction curves. Interpolate linearly for unlisted values.

For consistency of units, refer to Sec. 1.4.

Table 3.6 Correction Factors for Flexural Effective Width Coefficients, λ_f/λ_{f_0}, for Varying Aspect Ratios and Transverse Relative Column Size

	c_2/L_2			
L_1/L_2	0.03	0.06	0.12	0.18
0.50	0.917	1.000	1.168	1.337
0.75	0.936	1.000	1.126	1.253
1.00	0.950	1.000	1.099	0.195
1.50	0.967	1.000	1.062	1.120
2.00	0.977	1.000	1.041	1.079
3.00	0.981	1.000	1.022	1.041

Note: Interpolate or extrapolate linearly for unlisted values. If correction factor yields a λ_f greater than 1.0, then the value of λ_f to be used should be 1.0, meaning the whole width of slab is effective in bending action.

For consistency of units, refer to Sec. 1.4.

Table 3.7 Axial Effective Width Coefficients, λ_{a_0}, for Varying Aspect Ratios and Longitudinal Relative Column Size

	c_1/L_1					
L_1/L_2	0.04	0.08	0.12	0.16	0.20	0.24
0.50	0.189	0.182	0.176	0.170	0.163	0.156
0.75	0.266	0.255	0.244	0.234	0.224	0.214
1.00	0.350	0.332	0.316	0.300	0.286	0.272
1.50	0.515	0.484	0.455	0.429	0.405	0.381
2.00	0.645	0.603	0.566	0.533	0.502	0.473
3.00	0.800	0.747	0.703	0.664	0.629	0.598

Note: $c_2/L_2 = 0.06$ for all values listed. For c_2/L_2 different from 0.06, the appropriate correction factors must be used. Interpolate linearly for unlisted values.

For consistency of units, refer to Sec. 1.4.

Table 3.8 Correction Factors for Axial Effective Width Coefficients, λ_a/λ_{a_o}, for Varying Aspect Ratios and Transverse Relative Column Size

	c_2/L_2		
L_1/L_2	0.03	0.06	0.12 and higher
0.50	1.061	1.000	0.955
0.75	1.027	1.000	0.979
1.00	1.015	1.000	0.988

For L_1/L_2 greater than 1.0, no correction for c_2/L_2 is necessary.

Note: Refer to Sec. 1.4 for consistency of units.

Table 3.9 Composite Stiffness for Varying Slab Aspect Ratio

$c_1/L_1 = 0.12$ $L_2 = 125.0$ $c_2 = 15.0$
$A_{BT} = 125.0$ $I_{BT} = 1302.1$ $t = 5.0$

L_1	Composite Stiffness, $M/E_s\theta_o$		
	Finite Element	Proposed Method	% Error
62.5	344	344	0.0
125.0	532	531	-0.2
187.5	259	259	0.0
250.0	206	206	0.0
312.5	170	169	-0.6
375.0	145	144	-0.7

Note: Refer to Sec. 1.4 for consistency of units.

Table 3.10 Composite Stiffness for Varying Relative Column Dimension

$L_1 = 125.0$ $t = 5.0$ $A_{BT} = 125.0$
$L_2 = 125.0$ $c_1 = c_2$ $I_{BT} = 1302.1$

c_1/L_1 $(=c_2/L_2)$	Composite Stiffness, $M/E_s\theta_o$		
	Finite Element	Proposed Method	% Error
0.04	270	270	0.0
0.08	304	303	-0.3
0.12	344	344	0.0
0.16	392	392	0.0
0.20	450	449	-0.2

$L_1 = 125.0$ $t = 5.0$ $A_{BT} = 125.0$
$L_2 = 125.0$ $c_2 = 15.0$ $I_{BT} = 1302.1$

c_1/L_1	Composite Stiffness, $M/E_s\theta_o$		
	Finite Element	Proposed Method	% Error
0.04	271	270	-0.4
0.08	304	302	-0.7
0.12	344	344	0.0
0.16	390	390	0.0
0.20	444	445	0.2
0.24	510	510	0.0

Note: Refer to Sec. 1.4 for consistency of units.

Table 3.10 (continued)

$L_1 = 125.0$ $c_1 = 15.0$ $A_{BT} = 125.0$
$L_2 = 125.0$ $t = 5.0$ $I_{BT} = 1302.1$
$e = 10.0$

	Composite Stiffness, $M/E_s\theta_o$		
c_2/L_2	Finite Element	Proposed Method	% Error
0.02	344	343	-0.3
0.04	343	342	-0.3
0.08	343	342	-0.3
0.12	344	344	0.0
0.16	345	345	0.0
0.20	347	347	0.0

Note: Refer to Sec. 1.4 for consistency of units.

Table 3.11 Composite Stiffness for Varying Beam Eccentricity

$L_1 = 125.0$ $c_1 = 15.0$ $A_{BT} = 125.0$

$L_2 = 125.0$ $c_2 = 15.0$ $I_{BT} = 1302.1$

$t = 5.0$

Eccentricity, e	Composite Stiffness, $M/E_s\theta_o$		
	Finite Element	Proposed Method	% Error
0.0	76	75	-1.3
5.0	143	142	-0.7
10.0	344	344	0.0
15.0	676	679	0.4
20.0	1137	1147	0.9

$L_1 = 125$ $c_1 = 10$ $A_{BT} = 78.3$

$L_2 = 125$ $c_2 = 6$ $I_{BT} = 1691.7$

$t = 5$

Eccentricity, e	Composite Stiffness, $M/E_s\theta_o$		
	Finite Element	Proposed Method	% Error
0.1	75	74	-1.3
1.0	77	76	-1.3
2.0	83	82	-1.2
2.5	86	85	-1.2
3.0	91	90	-1.1
6.0	139	137	-1.4
9.0	218	216	-0.9
12.0	187	186	-0.5
15.0	469	469	0.0

Note: Refer to Sec. 1.4 for consistency of units.

Table 3.11 (continued)

$L_1 = 150.0$ $c_1 = 18.0$ $A_{BT} = 61.7$

$L_2 = 100.0$ $c_2 = 6.0$ $I_{BT} = 740.6$

$t = 8.0$

	Composition Stiffness, $M/E_s\theta_o$		
Eccentricity, e	Finite Element	Proposed Method	% Error
0.5	118	116	-1.7
1.0	119	117	-1.7
2.0	124	122	-1.6
3.0	132	130	-1.5
6.0	175	172	-1.7
9.0	245	242	-1.2
10.0	274	271	-1.1
12.0	342	340	-0.6
15.0	466	466	0.0

Note: Refer to Sec. 1.4 for consistency of units.

Table 3.12 Composite Stiffness for Varying Slab Thickness

$L_1 = 125.0$ $c_1 = 15.0$ $A_{BT}/A_{sg} = 0.20$

$L_2 = 125.0$ $c_2 = 15.0$ $I_{BT} = 1302.1$

$e = 10.0$

	Composite Stiffness, $M/E_s\theta_o$		
Thickness, t	Finite Element	Proposed Method	% Error
1.0	100	100	0.0
2.5	184	184	0.0
4.0	276	276	0.0
5.0	344	344	0.0
7.5	548	548	0.0
10.0	819	818	-0.1
15.0	1649	1647	-0.1

Note: Refer to Sec. 1.4 for consistency of units.

Table 3.13 Composite Stiffness for Varying Beam Area

$L_1 = 125.0$ $c_1 = 15.0$ $t = 5.0$ $I_{BT} = 1302.1$
$L_2 = 125.0$ $c_2 = 15.0$ $e = 10.0$

Area, A_{BT}	Composite Stiffness, $M/E_s\theta_o$		
	Finite Element	Proposed Method	% Error
0.0	76	75	-1.3
62.5	243	242	-0.4
125.0	344	344	0.0
187.5	412	412	0.0
312.5	498	498	0.0

$L_1 = 150.0$ $c_1 = 18.0$ $t = 8.0$ $I_{BT} = 740.6$
$L_2 = 100.0$ $c_2 = 6.0$ $e = 10.0$

Area, A_{BT}	Composite Stiffness, $M/E_s\theta_0$		
	Finite Element	Proposed Method	% Error
0.0	117	116	-0.9
12.9	156	153	-1.9
25.7	190	186	-2.1
38.6	222	218	-1.8
51.4	252	248	-1.6
64.3	280	276	-1.4
77.1	306	303	-1.0
90.0	331	328	-0.9
128.6	397	395	-0.5

Note: Refer to Sec. 1.4 for consistency of units.

Table 3.14 Composite Stiffness for Varying Beam Moment of Inertia, I_{BT}

$L_1 = 125.0$ $c_1 = 15.0$ $t = 5.0$ $A_{BT} = 125.0$
$L_2 = 125.0$ $c_2 = 15.0$ $e = 10.0$

	Composite Stiffness, $M/E_s\theta_o$		
I_{BT}	Finite Element	Proposed Method	% Error
130.2	296	302	2.0
260.4	304	307	1.0
651.0	320	320	0.0
1302.1	344	344	0.0
2604.2	390	389	-0.3
5208.3	482	481	-0.2

Note: Refer to Sec. 1.4 for consistency of units.

Table 3.15 Composite Stiffness for Various Values of Controlling Parameters

L_1	L_2	c_1	c_2	t	e	A_{BT}	I_{BT}	Composite Stiffness, $M/E_s\theta_o$		
								Finite Element	Proposed Method	% Error
125.0	125.0	15.0	15.0	8.0	10.0	200.0	5333.3	740	738	-0.3
125.0	125.0	15.0	15.0	8.0	16.0	200.0	5333.3	1408	1407	-0.1
125.0	125.0	25.0	25.0	5.0	12.0	78.3	1691.7	491	491	0.0
125.0	125.0	10.0	6.0	5.0	10.0	116.0	1691.7	305	304	-0.3
125.0	125.0	10.0	6.0	5.0	10.0	145.0	1691.7	339	338	-0.3
125.0	125.0	10.0	6.0	5.0	10.0	143.1	1691.7	336	335	-0.3
250.0	250.0	10.0	6.0	5.0	12.0	78.3	1691.7	172	170	-1.2
250.0	250.0	20.0	12.0	5.0	12.0	78.3	1691.7	195	194	-0.5
125.0	250.0	10.0	12.0	5.0	12.0	156.6	3383.3	546	548	0.4
250.0	125.0	20.0	6.0	5.0	12.0	78.3	1691.7	187	186	-0.5

Note: Refer to Sec. 1.4 for consistency of units.

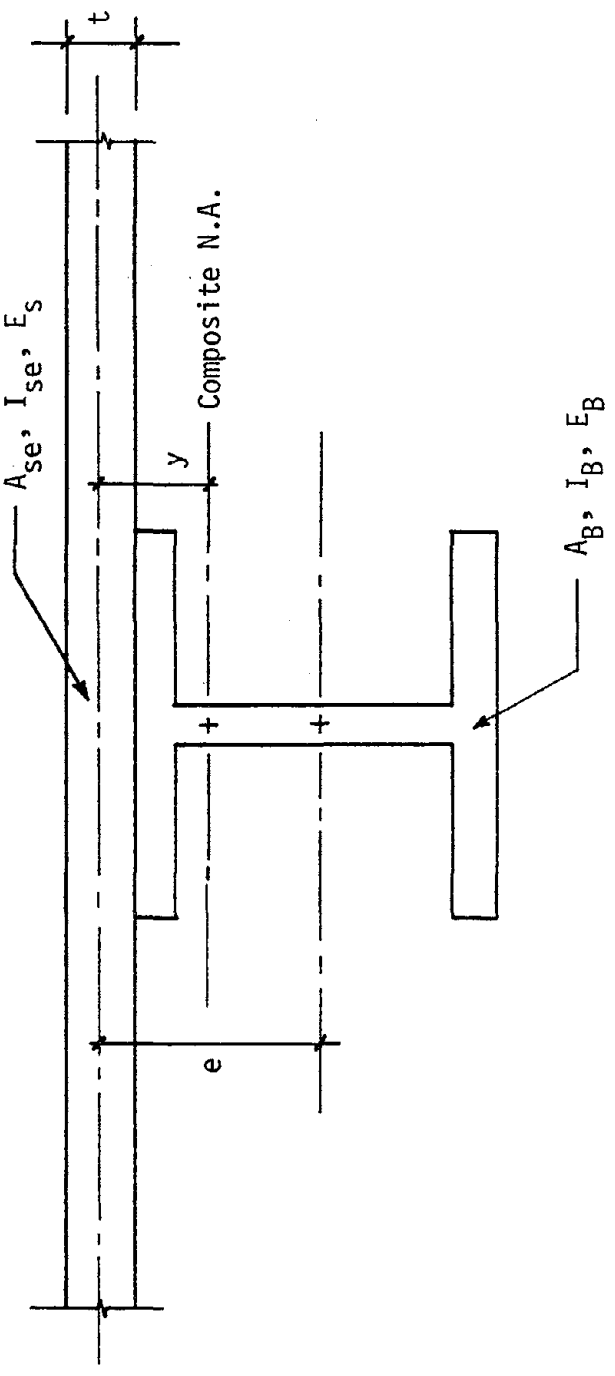

Fig. 2.1 Composite Section

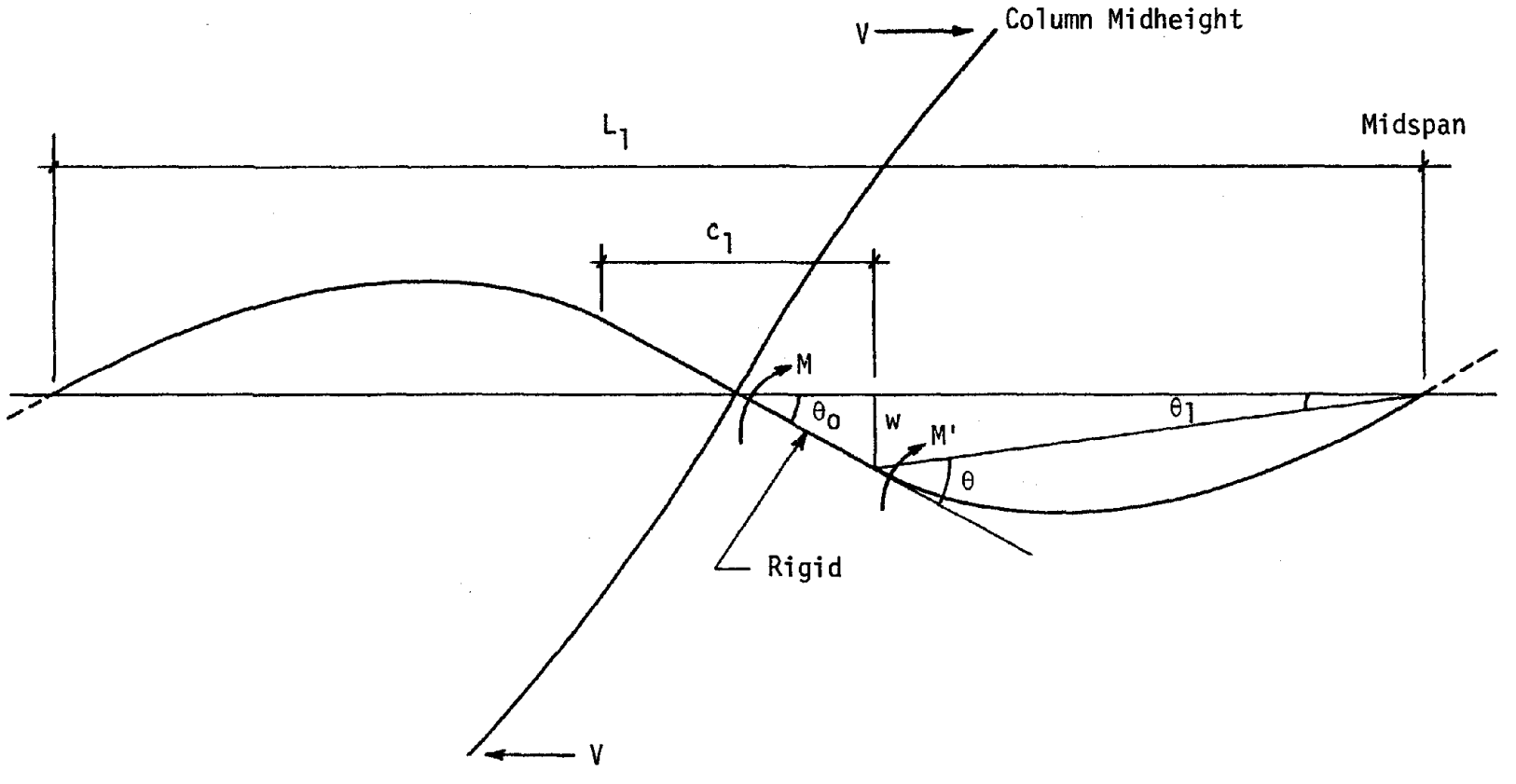

Fig. 2.2 Composite Beam in Antisymmetric Deflection

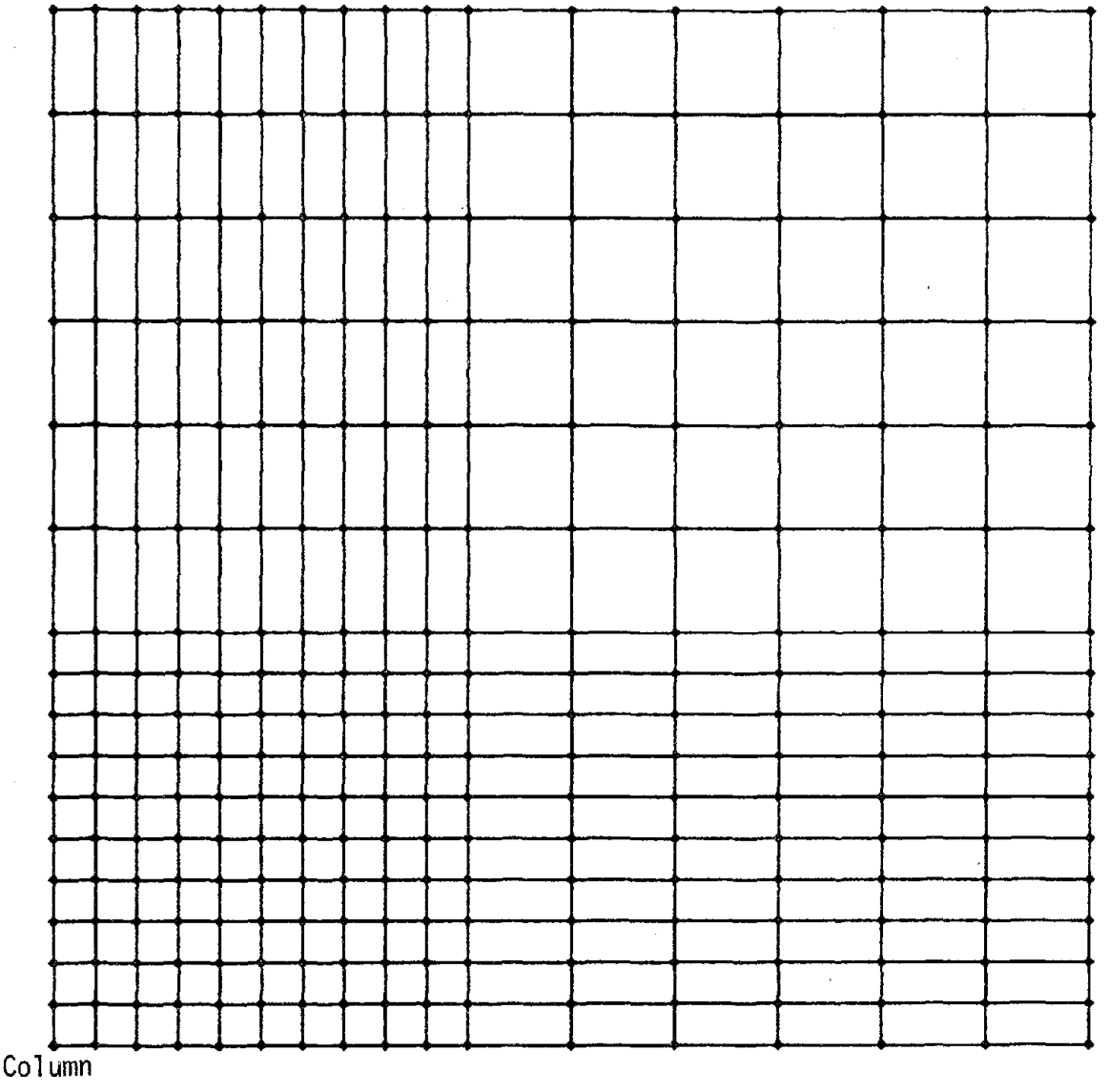

Fig. 2.3 The 16x16 Finite Element Mesh

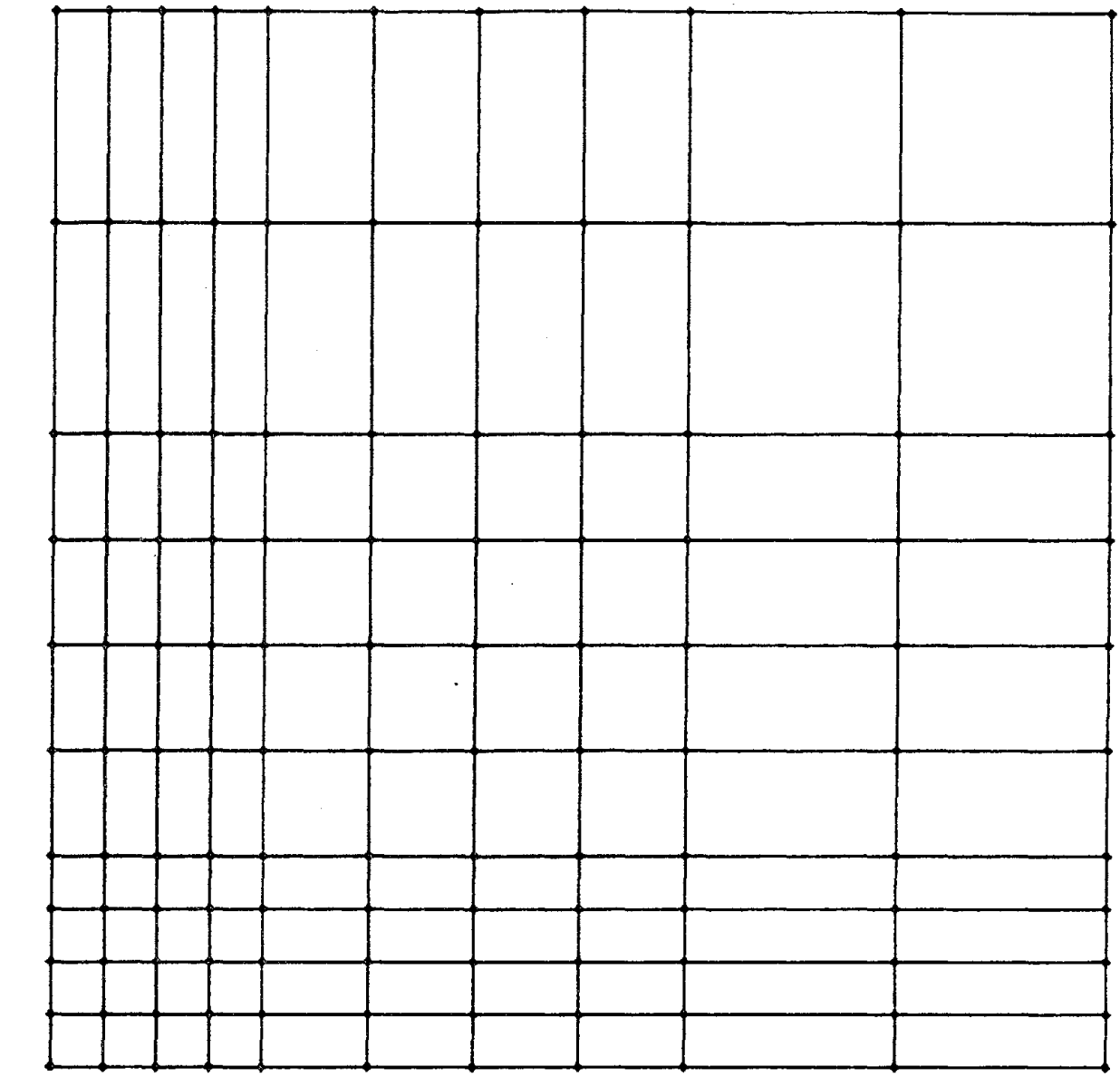

Fig. 2.4 The 10x10 Finite Element Mesh

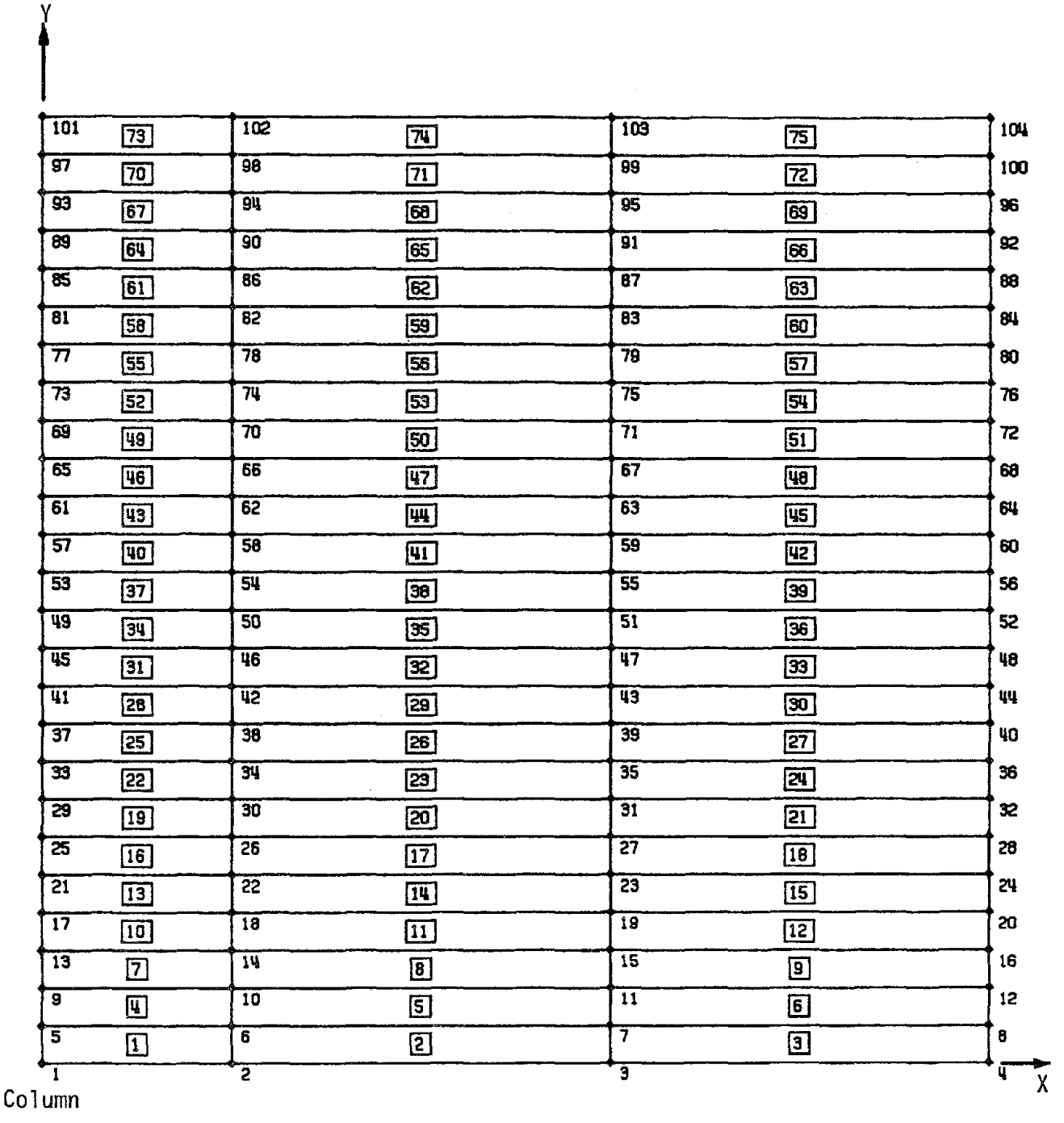

Fig. 2.5 The 3x25 Finite Element Mesh

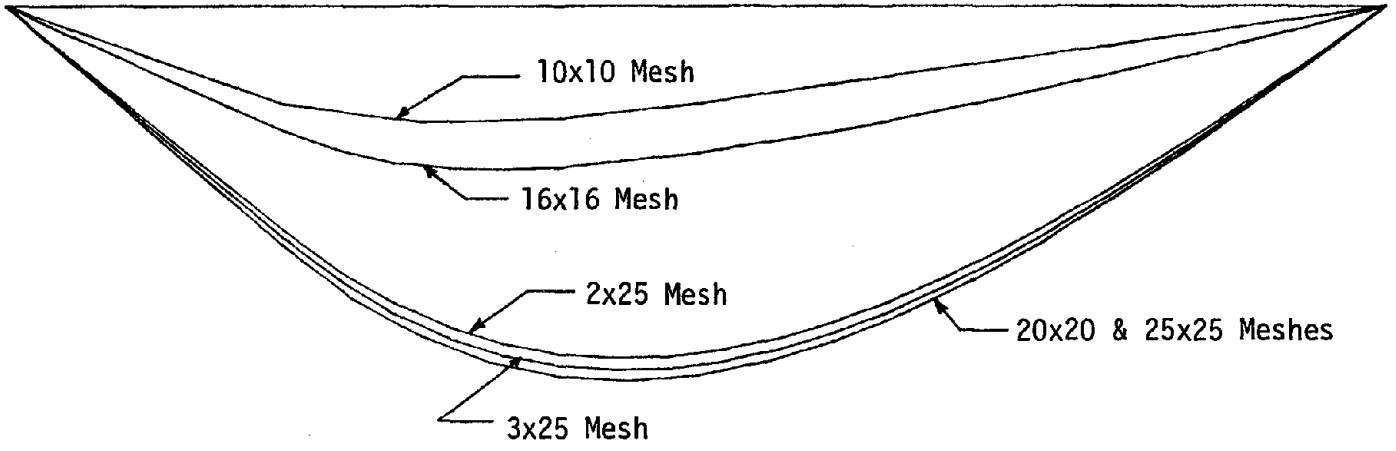

Fig. 2.6 Comparison of the Deflected Shape of the Composite Beam for Different Finite Element Meshes

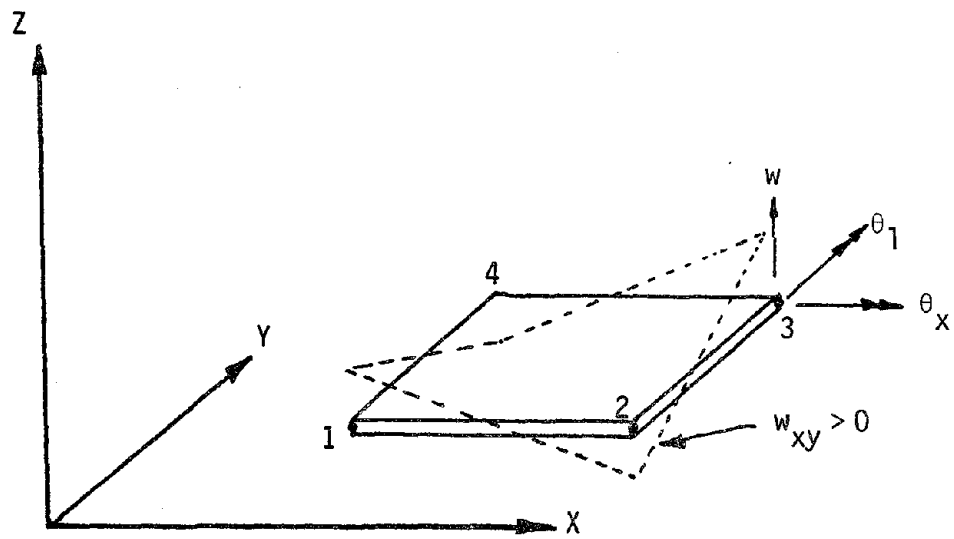

Fig. 2.7 Degrees of Freedom of the 16 Node Rectangular Plate Bending Element [24]

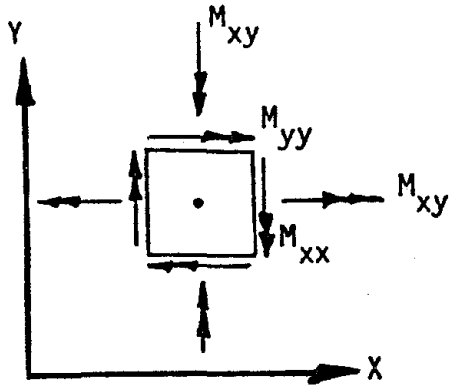

a) Positive Moments

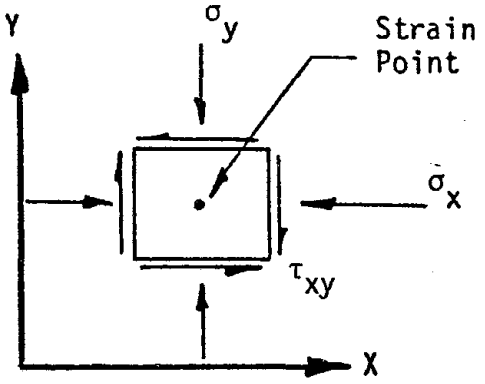

b) Stresses on Z > 0 Fibers for Positive Moments

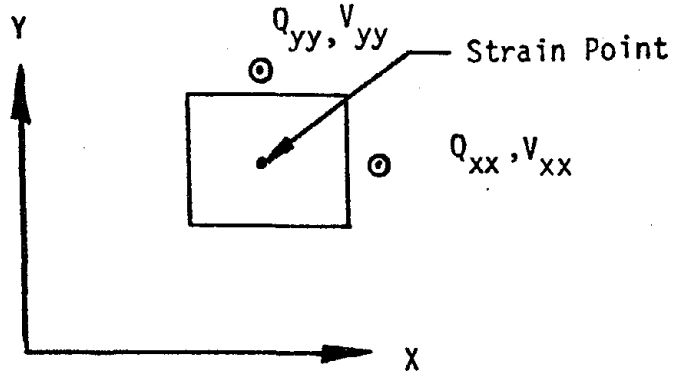

c) Transverse Shear Forces

Fig. 2.8 Generalized Stress and Strain Resultants for the Rectangular Plate Bending Element [24]

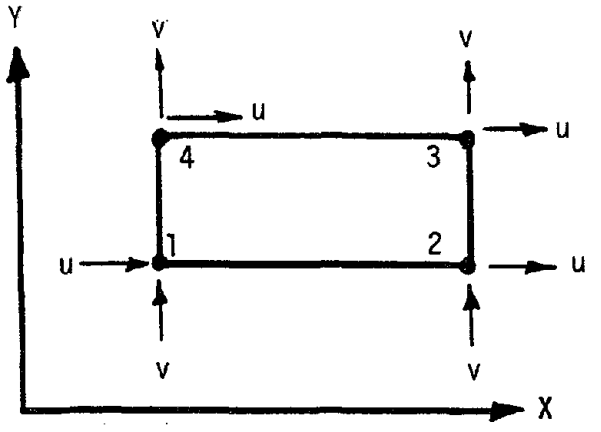

Fig. 2.9 Degrees of Freedom of the Plane Stress Rectangle [24]

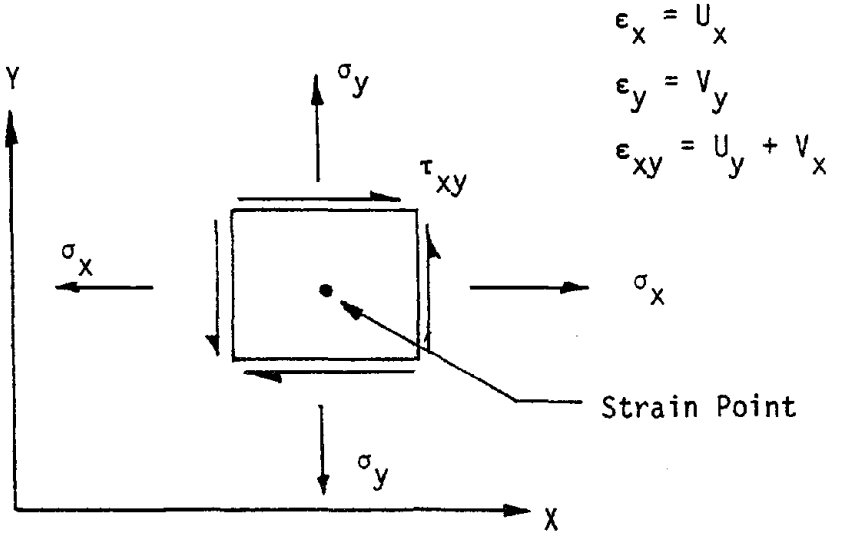

Fig. 2.10 Generalized Stresses and Strains for the Plane Stress Rectangle [24]

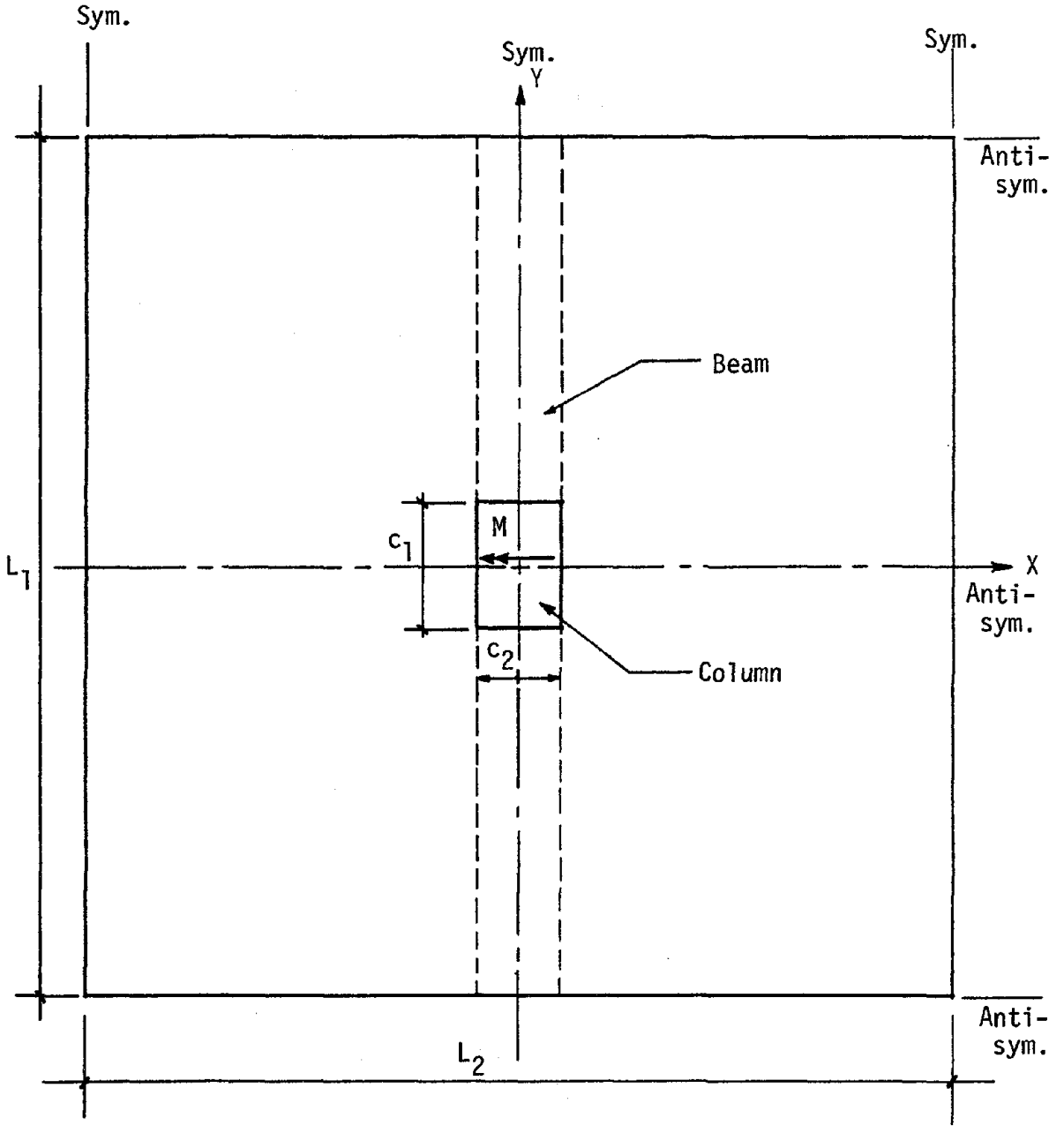

Fig. 2.11 Typical Interior Panel

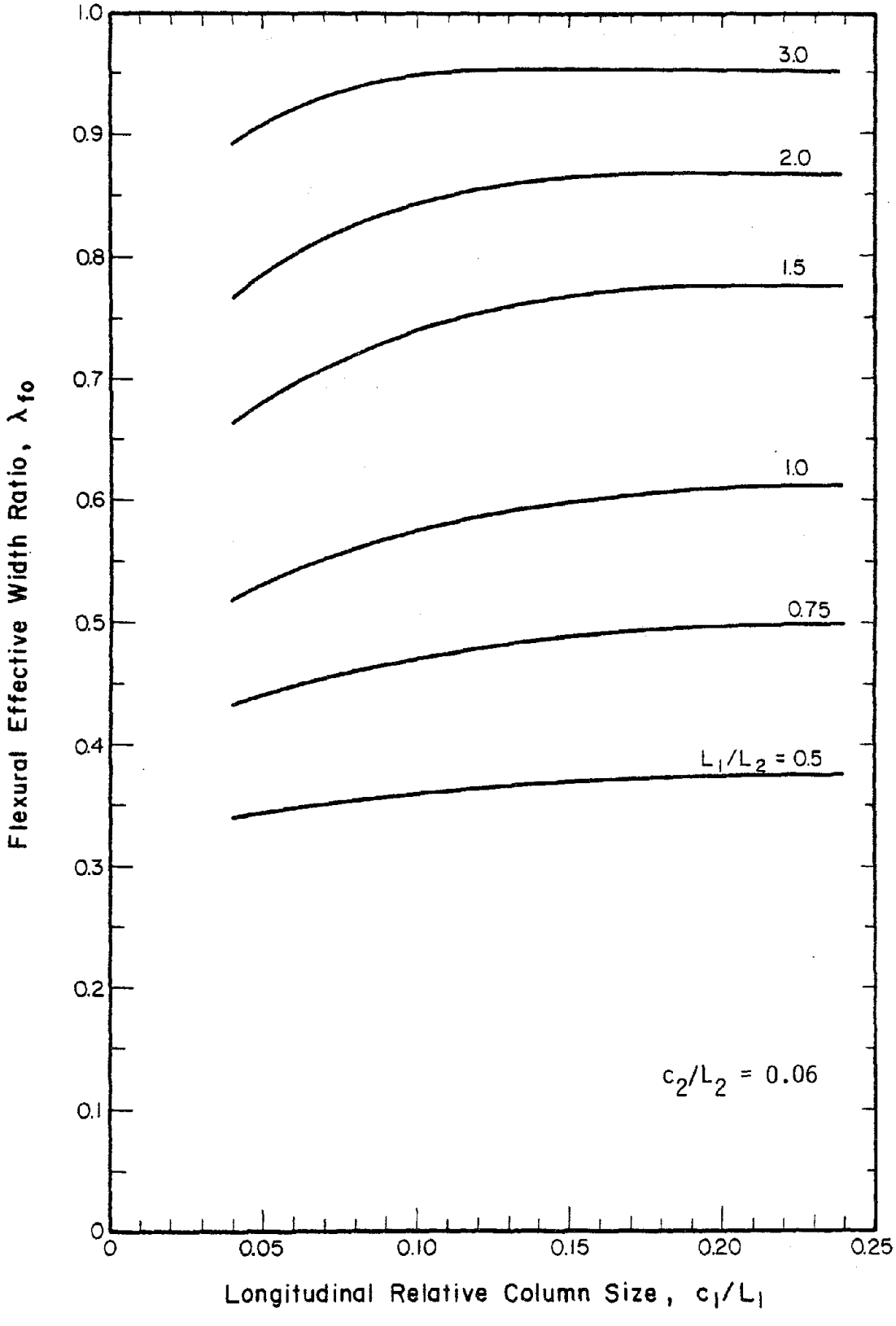

Fig. 3.1 Flexural Effective Width Ratios

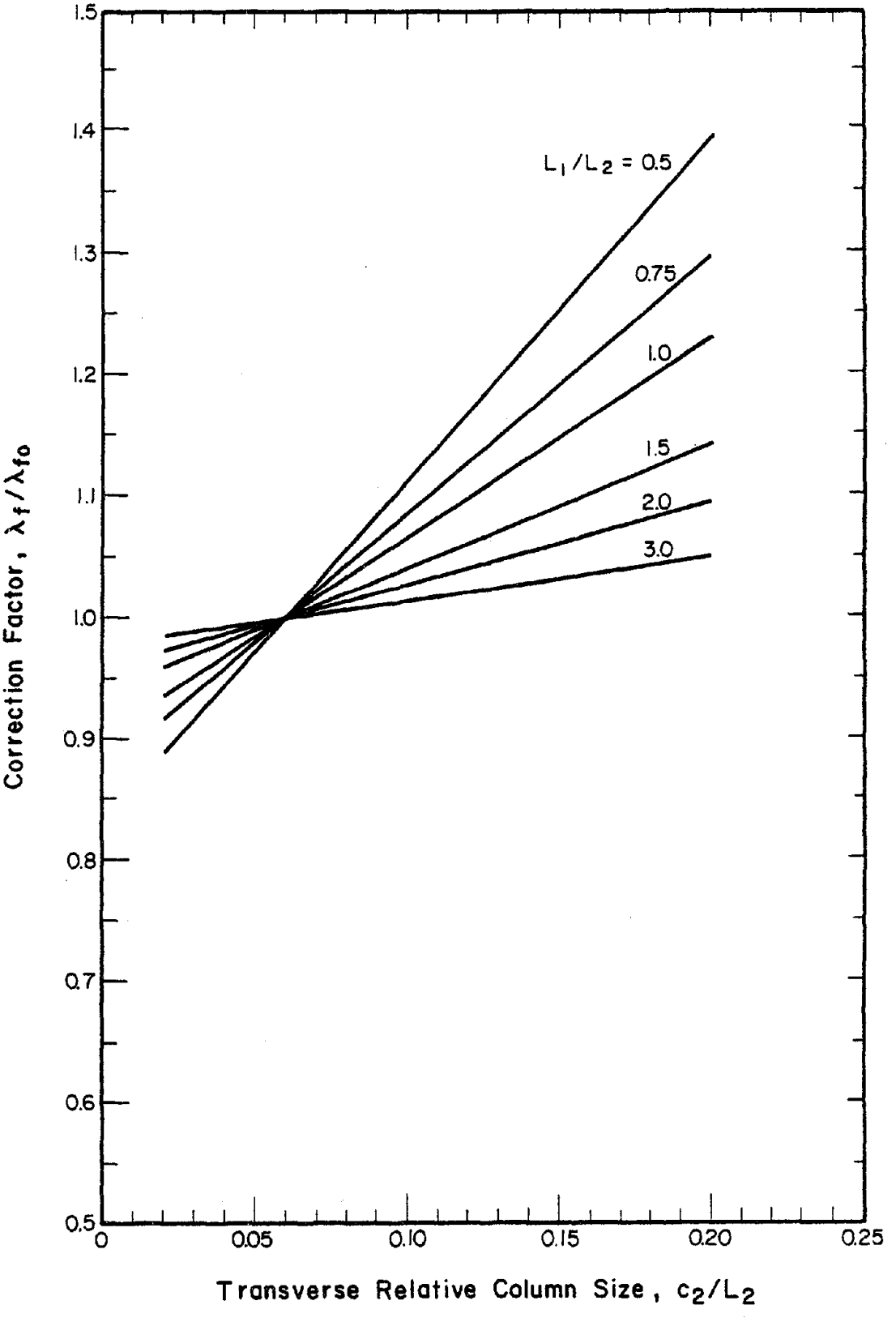

Fig. 3.2 Correction Factors for Flexural Effective Width Ratios

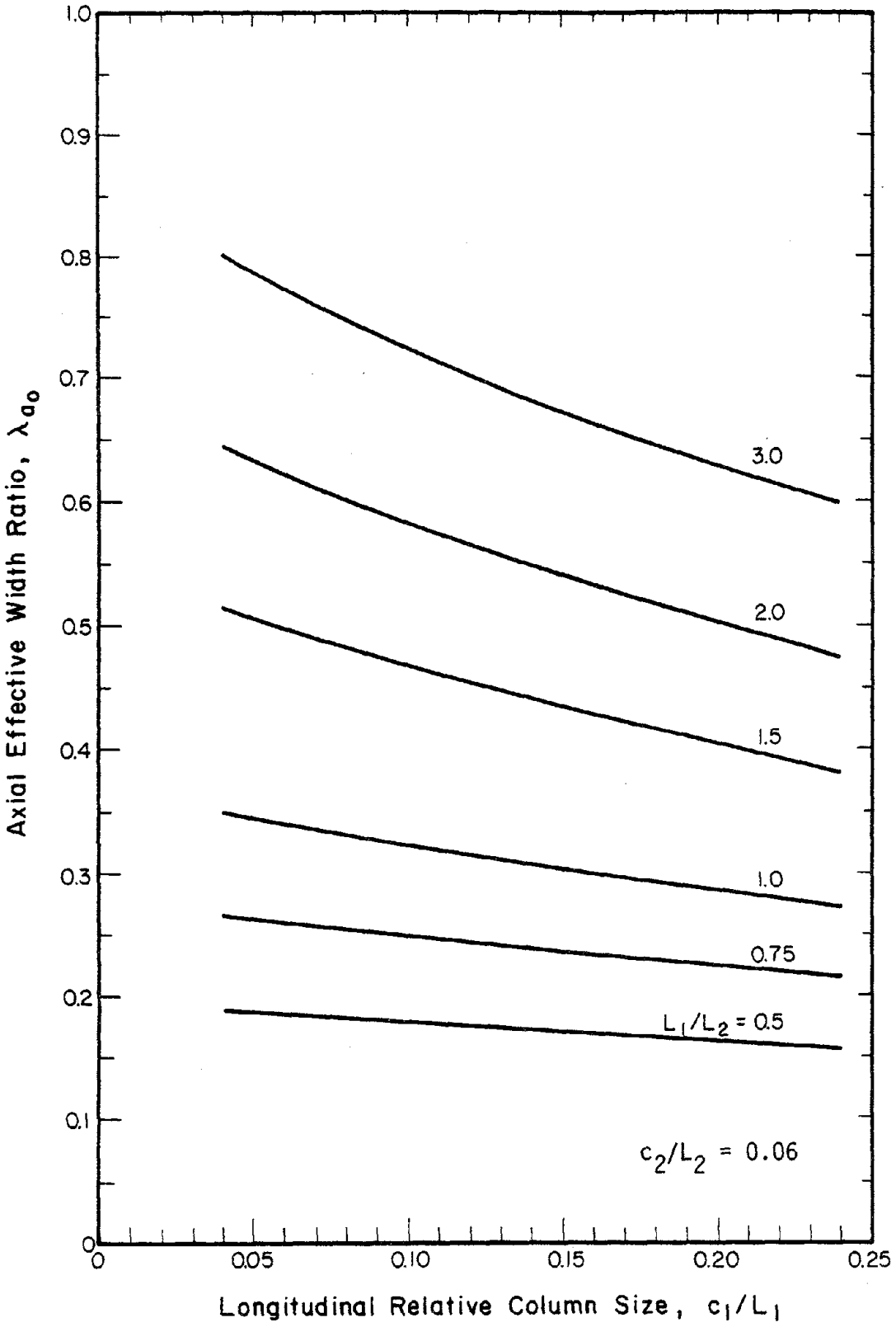

Fig. 3.3 Axial Effective Width Ratios

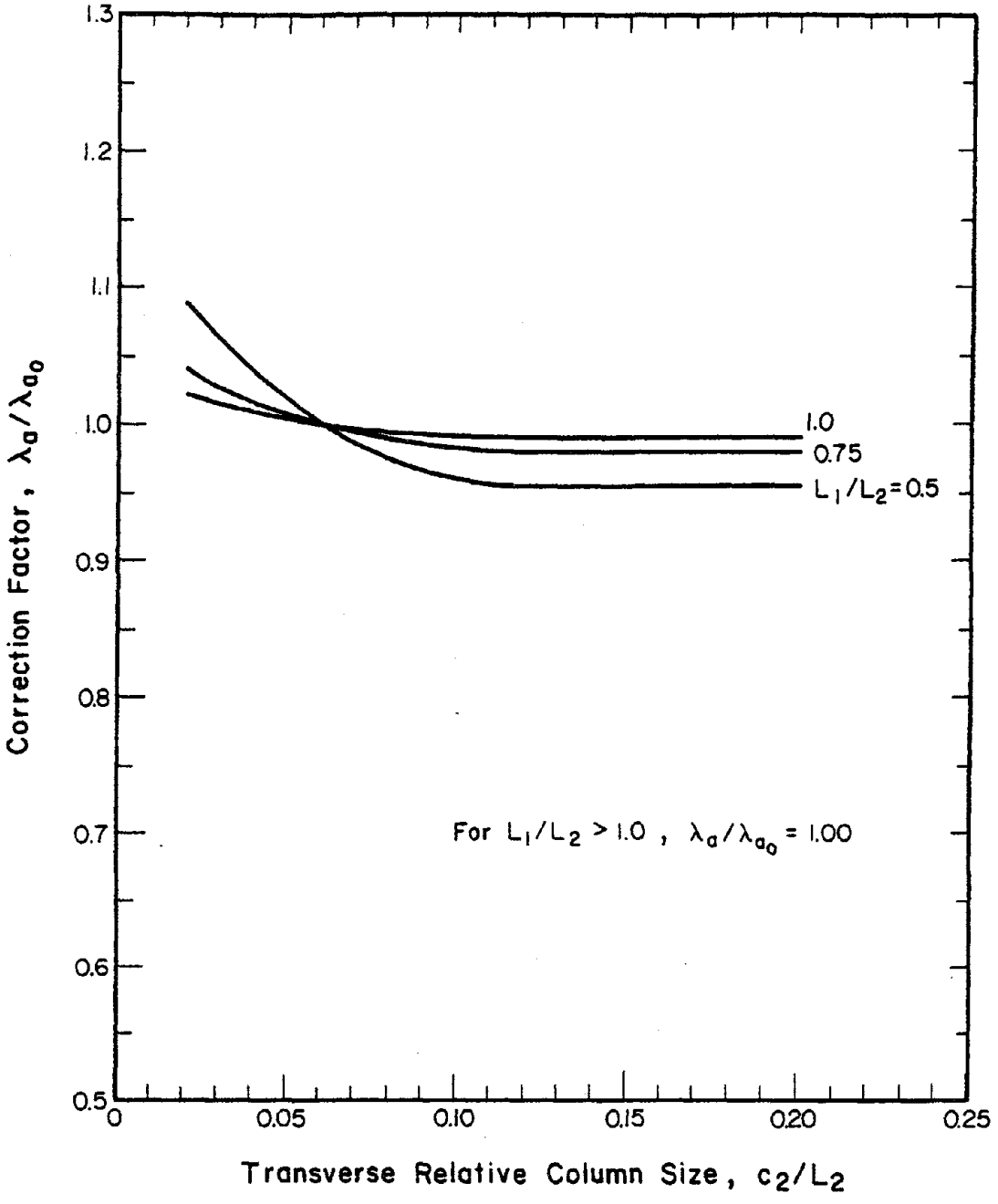

Fig. 3.4 Correction Factors for Axial Effective Width Ratios

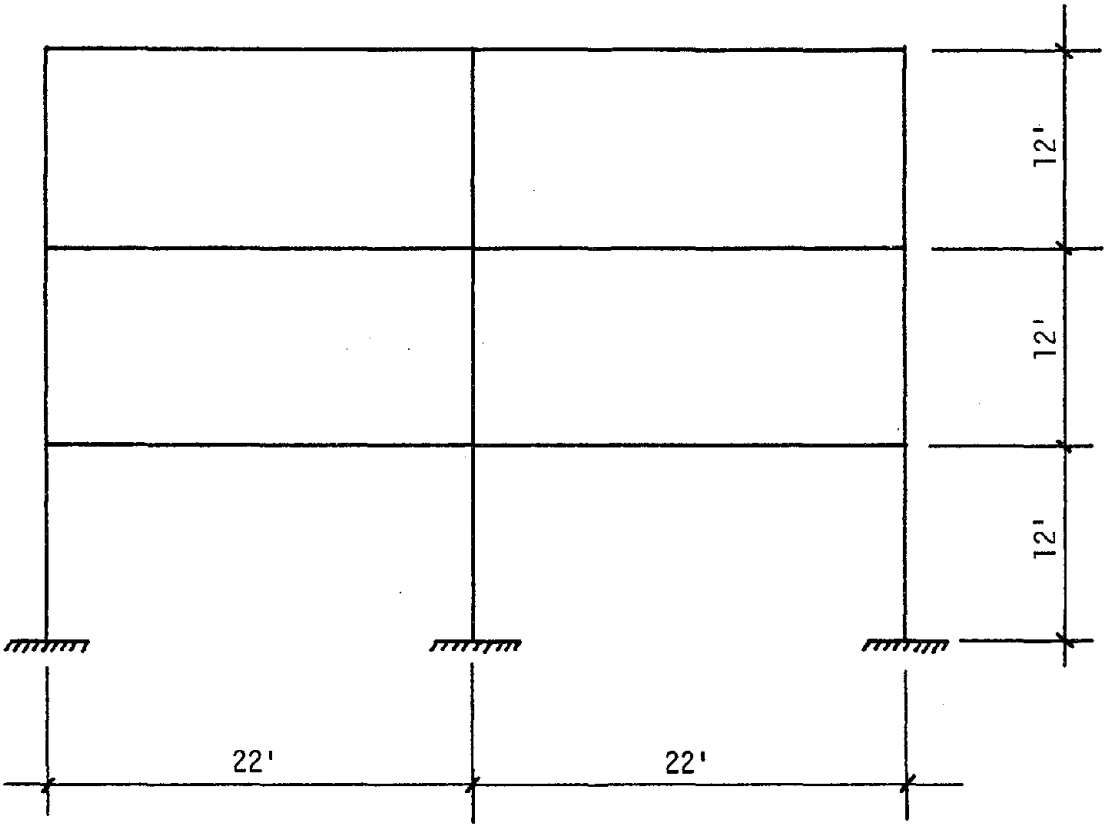

Columns: W14x127 (A36)
Beams : W21x68 (A36)
Slabs : 6" RC f'_c = 3500 psi
Transverse span = 20'

Fig. 4.1 Three-story Frame

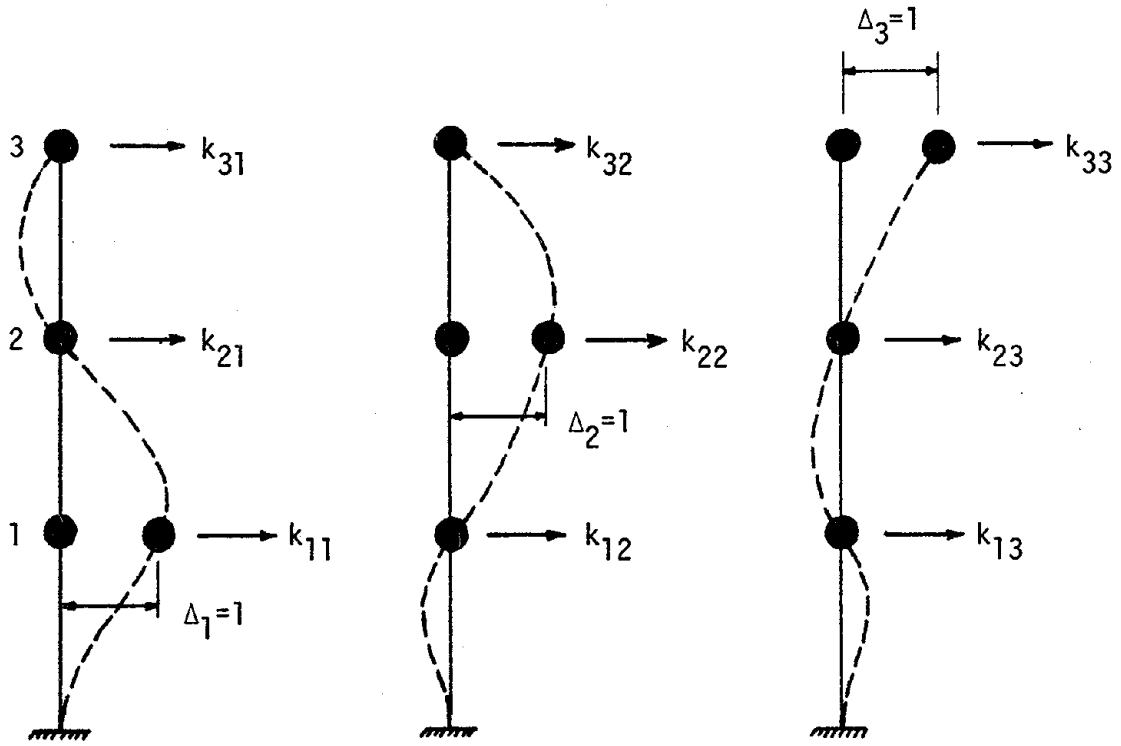

Positive Directions Illustrated

Fig. 4.2 Lateral Stiffness Coefficients

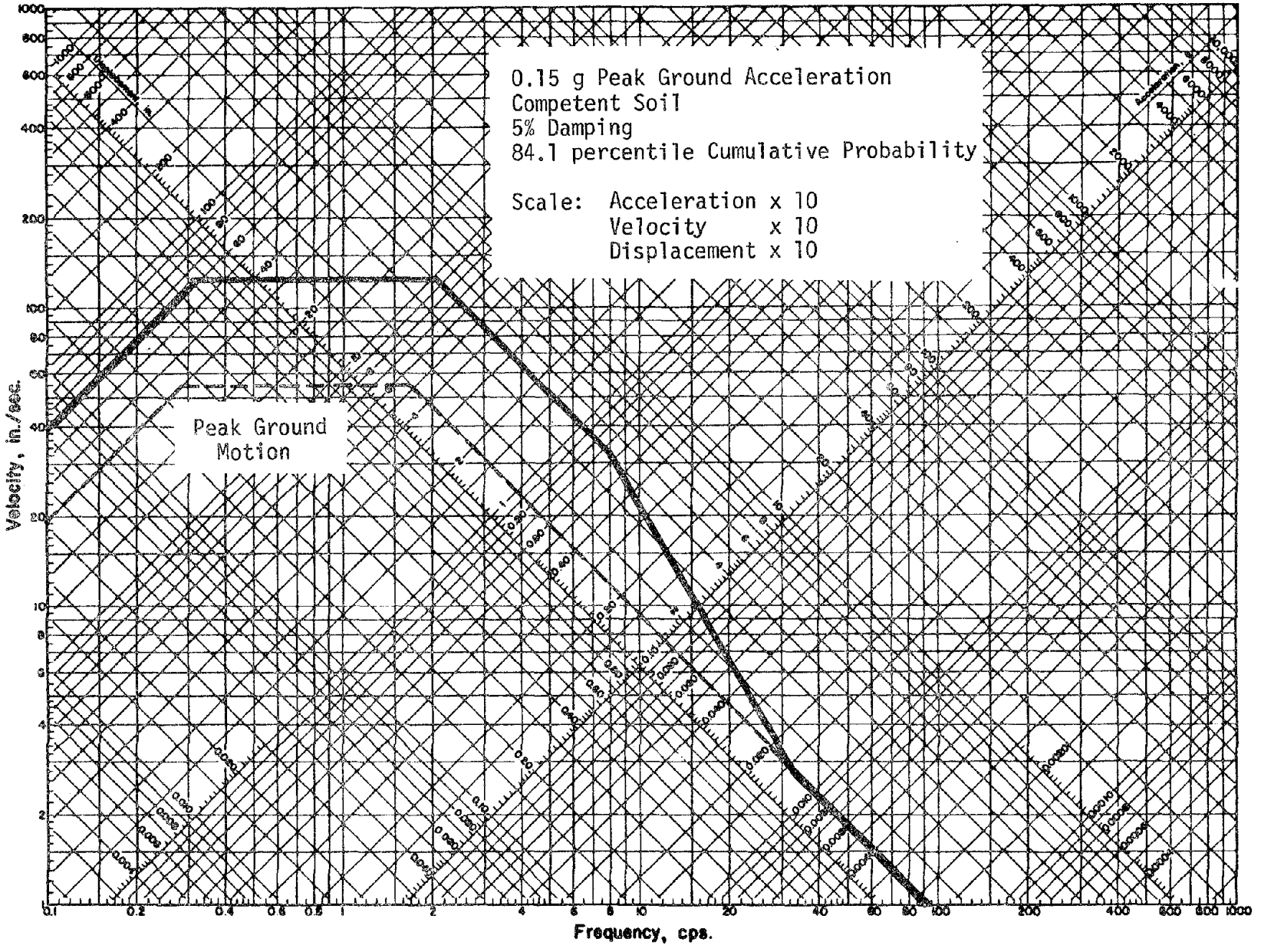

Fig. 4.3 Response Spectrum Used in Example 2